



International Erasmus Mundus Master in
QUATERNARY AND PREHISTORY



**Sedimentary facies and Soil Micromorphology of Gran
TD-10 units.**

Lila Warnitz

Supervisor: Josep Vallverdú

Co-supervisor: David M. Martín-Perea

Academic year 2022/2023



Abstract

This master's thesis is a study of the soil micromorphology of sediment samples taken between 2013 and 2022 from the TD-10 units at Gran Dolina (Atapuerca, Burgos, Spain). Gran Dolina is one of the most important sites present at Atapuerca. Several occupation layers have been discovered inside this site, including two in TD-10 units. This unit is therefore being studied in depth in order to gain a better understanding of its depositional context, both sedimentary and environmental, and its post-depositional evolution (e.g. taphonomy).

Although numerous studies have been carried out on the TD-10 units (e.g. facies definition and description, micro-vertebrate and pollen studies, chronological investigation...) several problems remain. In addition to the presence of two discontinuities within this stratigraphy, which poses a problem, the environment and in particular the variations in climate of this layer remain unclear. This study uses a soil micromorphology approach and analysis to understand the different facies which compose this layer and the climatic record associated.

The result of the investigation shows that Gran Dolina TD-10 layer is composed of three facies types, 1) Rhythmic very fine gravelly mud or muddy very fine gravel lamina set; 2) Rhythmic sandy mud to fine gravelly mud in fine bed-set facies; 3) Sandy mud in fine lamina set. Those different facies are mostly associated to grain and debris flow transport processes. Other types of deposits like solifluction and small rock fall were also detected and constitute an important part of TD-10 post-depositional features. In addition, the analysis of the different types of soil and soil features have allowed to establish that Gran Dolina TD-10 layer was formed during a succession of cold periods with different degrees of intensity interspersed with warmer and more humid periods.

Key words: Micromorphology; Facies; Climatic data; mode of deposits; Gran Dolina TD-10

Tables of contents

Abstract	2
List of Figure	4
List of Table	5
Chapter 1: Introduction	6
General presentation	6
Aims and Objectives	7
Sites presentation	7
The Sierra de Atapuerca	8
Geological Context of Atapuerca	8
Gran Dolina	9
Chapter 2: Set of Art	15
Gran Dolina TD-10 layer	15
Previous Research on the Geological Depositional Context of TD-10 units	15
Dolina TD-10 Units, Previous Sedimentary Facies Description Research	19
Chapter 3: Material and method	22
Thin section preparations:	22
Thin section observation and description	27
Chapter 4 : Result	31
4.1 General Characteristic of the facies and microfacies.	31
4.2 CLASSIFICATION OF THE FACIES	31
4.2.1 Rhythmic very fine gravelly mud or muddy very fine gravel lamina sets (Facies 1):	31
4.2.2 Rhythmic sandy mud to fine gravelly mud in fine besets (Facies 2)	40
4.2.3 Sandy mud in fine lamina-set (Facies 3)	45
4.3 TD 10 Resume- Stratigraphy	52
Chapter 5: Discussion	54
Stratigraphy to paleo-stratigraphy	54
TD-10 unit Soil horizon	54
TD-10-unit Soil Sequences and Classification	58
TD-Unit Palaeoenvironment data	63
Soil data and MIS correlation	63
TD-10 unit micro-vertebrate reconstruction	64
TD-10 unit Palynology reconstruction	65
Chapter 6 : Conclusion	67
Acknowledgements	69
Bibliography	70
Annexes 1	85

List of Figure

FIGURE 1: MAP SHOWING THE LOCALIZATION OF ATAPUERCA	9
FIGURE 2: BAYESIAN MODEL DATES OF TD-10 UNIT CORRELATES WITH THE MARINE ISOTOPIES STAGES	11
FIGURE 3: STRATIGRAPHIC UNITS PROPOSED FROM TD-10 OF GRAN DOLINA SITE BASED ON FIELD OBSERVATION-SINTHETIC LOGS FROM SITE OUTCROPS WITH THE POSITION OF THE SAMPLES FOR SOIL MICROMORPHOLOGY AND PETROGRAPHIC STUDIES INCLUDED IN THIS MTH.....	13
FIGURE 4: DRYING FURNACE	24
FIGURE 5: WATER JET SAW	24
FIGURE 6: VACUUM CHAMBER	24
FIGURE 7: BOUNDING UNITS (PHOTO-OPEYEMI ADEWUMI, 2019)	25
FIGURE 8: MULTIPLE GRINDER MACHINE WITH A) GENERAL VIEW OF THE MULTIPLES GRINDER MACHINE, B) GRINDER SYSTEM	26
FIGURE 9: FINAL THIN SECTION OF A THICKNESS OF 30 MICRON (PHOTO-OPEYEMI ADEWUMI, 2019)	27
FIGURE 10: PHOTOGRAPHY OF PEDOFEATURES	32
FIGURE 11: HALOTYPES OF THE FACIES 1:.....	33
FIGURE 12: PHOTOGRAPHY OF PEDOFEATURES 2	39
FIGURE 13: HALOTYPES OF FACIES 2	42
FIGURE 14 LINK CAPPING PEDOFEATURES.....	44
FIGURE 15: HALOTYPES OF FACIES 3	47
FIGURE 16: PHOTOGRAPHY OF PEDOFEATURES 3	51
FIGURE 17: STRATIGRAPHY LEGEND OF THE COLUMNS N12 (A), N16/N17 (B) AND K22 (C) OF GRAN DOLINA TD-10	52
FIGURE 18: GRAN DOLINA TD-10 STRATIGRAPHY OF THE COLUMNS N12 (A), N16/N17 (B) AND K22 (C)	53
FIGURE 19: SCHEMA OF SOIL HORIZON ORGANISATION	54
FIGURE 20: PEDOSTRATIGRAPHY OF GRAN DOLINA TD-10 OF THE COLUMNS N12 (LEFT), N16/N17 AND K22 (RIGHT)FIGURE 20: PEDOSTRATIGRAPHY OF GRAN DOLINA TD-10 OF THE COLUMNS N12 (LEFT), N16/N17, AND K22 (RIGHT).....	62
FIGURE 21 "DISTRIBUTION OF THE EARLY MIDDLE PLEISTOCENE HABITATS OF SMALL-MAMMAL ASSOCIATION THOUGHOUT THE GRAN DOLINA SEQUANCE, SIERRE DE ATAPUERCA, BURGOS, SPAIN	66

List of Table

TABLE 1 LABELLED MONOLITHS EXTRACTED FROM UNIT TD 10 IN GRAN DOLINA, ATAPUERCA (SPAIN), YEARS 2022 AND THEIR LENGTH ASSOCIATED.....	23
TABLE 2: THIN SECTION LABELLED USED IN THIS STUDY, THEIR NUMBERS ASSOCIATED AND WITH THEIR STRATIGRAPHIC LEVEL.....	29
TABLE 3: LISTING AND DEFINITION OF THE DIFFERENT MASTER HORIZONS, GRADATIONS AND SUBORDINATES FIND OR NEED TO DEFINE THE HORIZON PRESENT INSIDE TD-10 UNITS.....	56
TABLE 4 : CORRELATION BETWEEN THE FACIES DEFINED INSIDE THE CHAPTER 3 AND THE DIFFERENT SOIL SEQUENCES	60

Chapter 1: Introduction

General presentation

The micromorphology is the study of burial soil in their undisturbed form at a microscopic level. This includes the study of all the related material at a microscopic level (Stoops George, 2003). It is a part of the geology study field, and it uses to understand and analyse the genesis, the classification and the management of the soil (Stoops George et al., 2010). Studies using micromorphology cover a wide range of subjects, from the analysis of agricultural soils to improve their yield to the investigation of archaeological sites.

Even if we can place the start of micromorphology at the early 20th century (Delage & Lagatu, 1904), the first major advance in this disciplinary happens in 30s years with the publication of Kubiena's book "micro pedology" (1938). The term of micromorphology was then introduced by the same authors in his following study and writing (W. L. , Kubiëna, 1953; W. L. Kubiëna, 1948) The second major advance arrives during the 60s years. In that time, technical progress allows prepared thin sections in a more efficient and easy way (Altemüller, 1962; Borchert, 1961; Jongerius & Heintzberger, 1962), and therefore makes micromorphology more accessible. Despite the continuous progress of thin section preparation techniques in micromorphology (Guilloré, 1980), its application of for archaeology context remains rare (Bronnikova et al., 2016). The first text of micromorphology in archaeology, "Soil and micromorphology in Archaeology" (Courty et al., 1989) is published in the start of the ninety. All this reason can explain why the micromorphology is considered as a young disciplinary, particularly in archaeology where this type of study, although a definite increase, is still not widespread (Bronnikova et al., 2016).

Today, micromorphological analyses as part of archaeological studies are used in two major cases: to understand the human influence on local or regional soil formation; and to obtain information of palaeoenvironment (e.g. regional landscape evolution, climate evolution). (Macphail & Gildberg, 1995) . This study belongs to the last category.

The micromorphology is a very powerful tool to understand the soil formation and processes (Sageidet, 2000). This includes all the environmental data that palaeosols can contain, but also they used as stratigraphic markers. To extract this data, it is imported to formulate two initial hypotheses. Firstly, it should be considered that all the pedological features formed by past pedogenic processes are comparable to those formed by the same modern process. And secondly,

we must assume that some pedofeatures and processes are specifically associate to with some environment (Birkeland, 1984).

Therefore, palaeosol and micromorphology analysis can contribute to the Quaternary studies. They can be particularly interesting for the site presenting a little or contradictory information.

Thus, this master thesis seeks to provide information on the environments that compose the TD-10 layer of Gran Dolina and its evolution. Previous study on micro-vertebrates and pollen have already established that this layer of the site has faced change of environments (e.g. (Cuenca-Bescós et al., 2011; Cuenca-Bescós & García, 2007)). Despite, the succession of those environments has not yet been fully understood, especially the climate condition of this layer formation. The precise determination of the general environments conditions and it climates is important as TD-10 units of Gran Dolina present human occupation remain. The better the environments will be understood, the better the condition of human occupation, but also its evolution will be known.

Aims and Objectives

The aim of this thesis is to carry out an in-depth study of the TD-10 layer at the Gran Dolina site (Atapuerca, Burgos, Spain).

In order to achieve this aim, the following objectives have been defined

- 1) Determine the different modes of deposition making up layer TD-10 in order to understand its organization, and obtain a detailed stratigraphy of this layer. For this, the paper by Bertran et al (1999), and Blikra (1998) were used as a reference.
- 2) Determine the nature of the soils, sequences and phases present, in order to use them as markers of the different potential environments of the TD-10 layer.
- 3) Determined the soil formation processes, in order to understand the factors involved in soil formation.

Sites presentation

The sites study inside this master thesis is Gran Dolina, one of the most important sites inside Atapuerca.

The Sierra de Atapuerca

The Sierra de Atapuerca is a hill located at 14-15 km east of the Burgos City inside the autonomous community of Castilla y León (Spain) (Figure 1.A)(Ortega et al., 2017). It presents an important Karstic system, which has created a lot of galleries and caves with archaeology remains inside. Since its discovery in the 19th century, it has revealed dozens of archaeological sites from the early Pleistocene to the present day. Some of them are among the most important prehistoric sites in Europe. It is the case of Gran Dolina, which is the site of this research, but also Siema del Elefant or Siema del Huesos.

Atapuerca sites can be devised in two parts, the sites of the “Trinchera del Ferrocarril”(TF), and the one of the “Cueva Mayor”. The most important site of the TF section is Gran Dolina (Carbonell et al., 1999).

Geological Context of Atapuerca

The Sierra Atapuerca is an anticlinal formation composed of limestone dating from the Mesozoic (Olivé et al., 1990; Pineda & Arce, 1997). It runs NNW-SSE with an NE orientation. The karstic systems from which the various archaeological sites originate are formed by the more modern layers of the anticline (Upper Cretaceous) composed of calcarenites, limestone, marly limestone, dolomites and marls. It is positioned at the most north-western part of the Iberian chain, at the junction of different Sierra (Montagne/hill), Sierra de la Demanda in the south and Sierra de Ubierna, Penahoradada and Temino at the north, inside the Duero Basin (Figure 1.B) (Pineda, 1997). In addition, it presents a multi-level system, compose of three sub-horizontal levels (Ortega, 2009; Ortega et al., 2013). Gran dolina is present at the intermediate level of this system (Campaña et al., 2017).

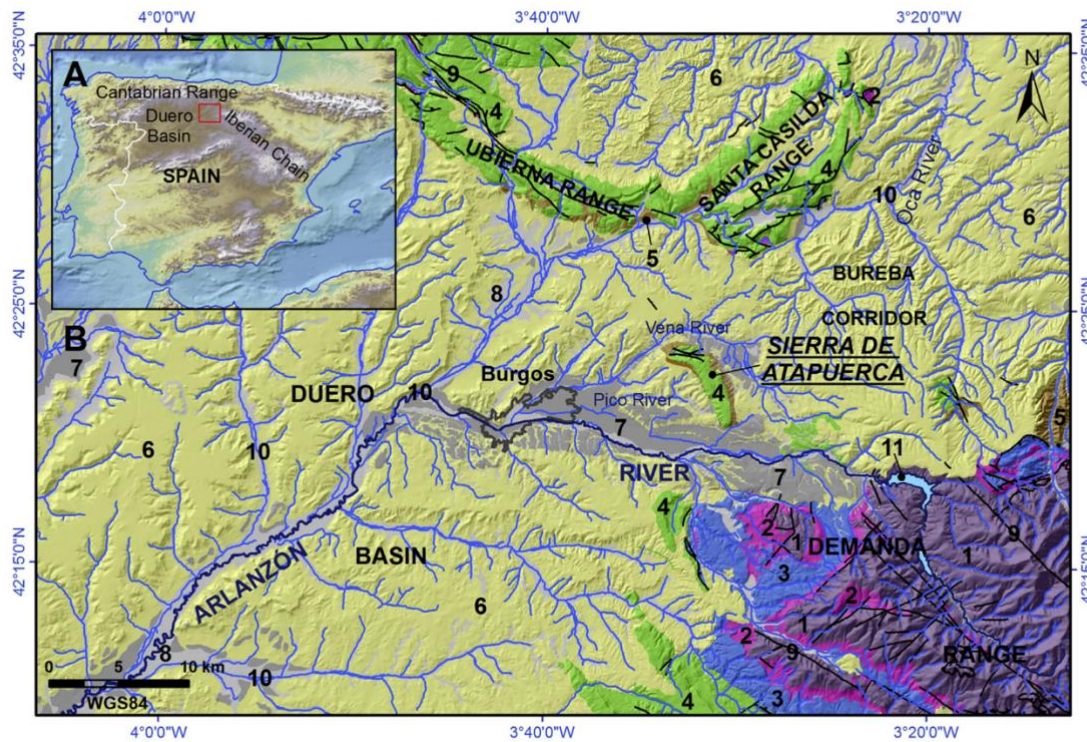


Figure 1: Map Showing the Localization of Atapuerca

Figure extracts from extract from “ Palaeogeographical reconstruction of the Sierra de Atapuerca Pleistocene sites (Burgos, Spain) “fig 1 ” Study area framework. A) Situation of the NE Duero Basin in the Iberian Peninsula. B) Location of the Sierra de Atapuerca in the NE Duero Basin. Legend: 1, Palaeozoic; 2, Triassic; 3, Jurassic; 4, Cretaceous; 5, Oligocene-Early Miocene; 6, Miocene; 7, Pleistocene; 8, Holocene; 9, faults; 10, drainage network; 11, Reservoir” by Benito-Calvo et al., 2017

Gran Dolina

Gran Dolina is an ancient cave site completely filled with sediment. It presents an important stratigraphy, one of the most important of Atapuerca. Indeed, Gran dolina stratigraphy presents a profile of 19 m thick from the early Pleistocene to the late Pleistocene. It is divided into 11 lithostratigraphic levels, the Trinchera Dolina (TD), with TD-1 representing the bottom and the most ancient part of the stratigraphy and TD-11 the top and the most recent part of the stratigraphy (Gil et al., 1987; Parés & Pérez-González, 1999). From the bottom to the top, these units are divided into two categories, the units composed of autochthonous sediment (TD-1 and TD-2) and the units composed of allochthonous sediments (TD-3 to TD-11). Only the units TD-3 to TD-11 represent an archaeological interest, while the TD-1 to TD-2 are archaeologically sterile (Campaña et al., 2017).

This stratigraphy is mainly composed of mass flow and fluvial deposits with the formation of terra rossa soil in roof chimneys (Campaña et al., 2017). A lot of archaeological remains were found in all the stratigraphy of Gran Dolina, going from human remains to fauna fossils and pollen including

lithic industry. However, the Human remains were found in only two units of the site, TD-6 and TD-10. Those units are respectively dating from the early Pleistocene and the Middle Pleistocene.

TD10 Gran Dolina chronology and preliminary modelled Bayesian dates

Some statistical analysis was effectuated on previous published dates of TD-10, TD-9 and TD-11 (Moreno et al. 2015; Berger et al., 2008; Falguères et al., 1999), in order to be correlated the Marine Isotopique Stage (MIS) with the TD-10 unit.

Several, dates were picked for each subunit and TD-10 (TD-10.1, TD-10.2, TD-10.3 and TD-10.4), the top part of TD-9 and the bottom of TD-11. For each layer's dates, a preliminary Bayesian model was made thank to Oxcal software (Figure 2).

GRAN DOLINA TD10 DATES AND MIS CORRELATIONS v. july 2023

OxCal v4.4.4 Bronk Ramsey (2021); r:5

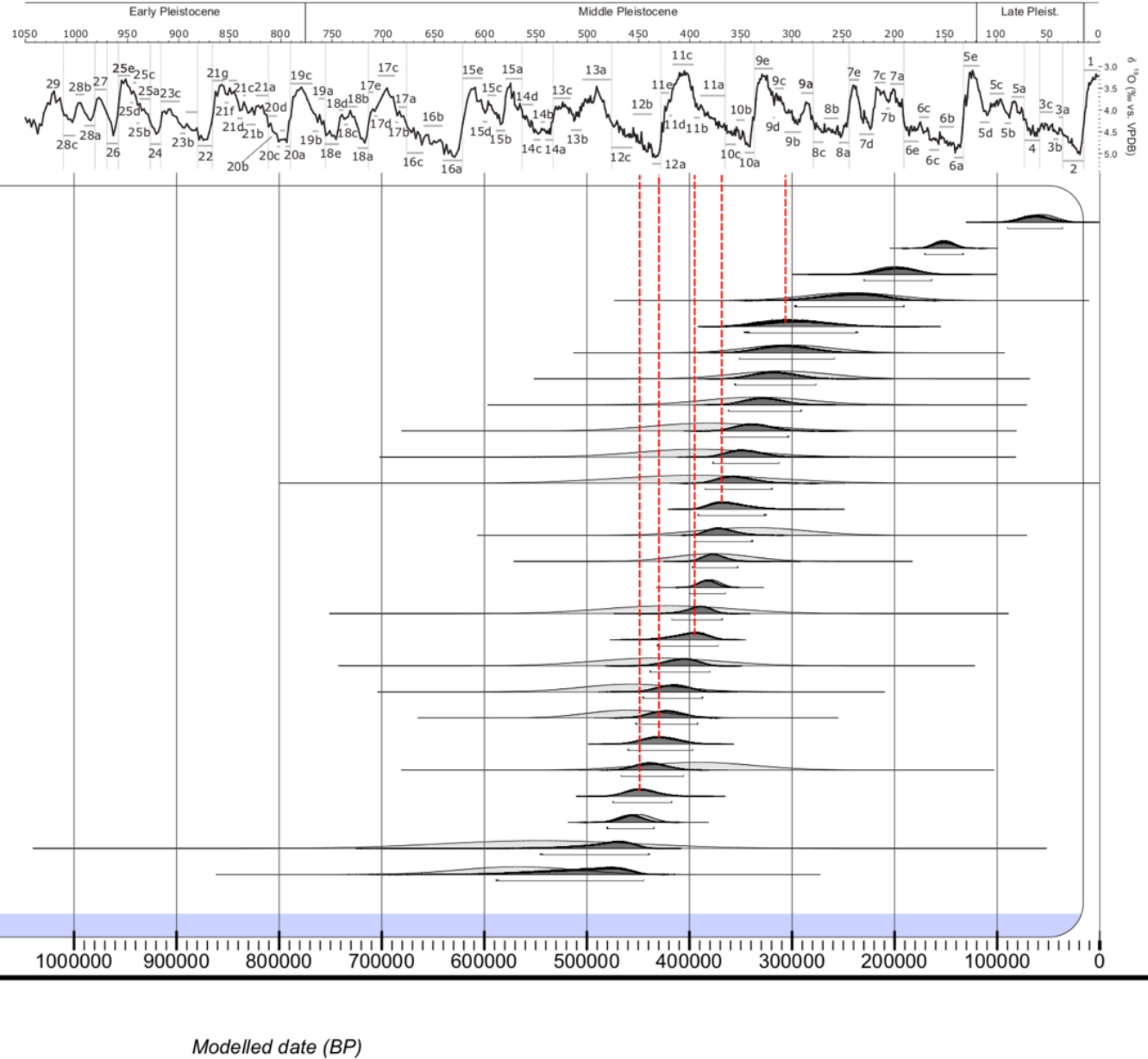


Figure 2: Bayesian model dates of TD-10 unit correlates with the Marine Isotopes Stages

In addition, the Bayesian model also gives the degree of reliability of the dates by their accuracy (e.g A:117)

According to the Figure 2, we can see that the TD-10 unit is associated to 5 MIS (red line) : MIS 12b, MIS 12a, MIS 11b, MIS 11a, and MIS 9c.

The MIS 12, coincide to a glacial inception, in which the MIS 12 a and b correspond to two glacial substages (Regattieri et al., 2016). It is also correlate the TD-10.4 subunit (Figure 2). During this period, we can note an important reduction of the precipitation, which has contributed to the decrease of lake levels but also to the increase of erosion (Regattieri et al., 2016). Therefore, we can assume that the climate associate to TD-10.4 must have been dry and cold, with the presence of erosion.

The MIS 11, encompasses the stratigraphic subunits 10.3 and 10.2, with MIS 11b connect to TD-10.3 and MIS 11a with TD-10.2. Globally, the MIS 11 is a warm stage associate to a global ice volume reduction. Its organization, correspond to one unique interglaciate and several interstadials (Candy et al., 2014). Indeed, the MIS 11b represent a short stadial event, while MIS 11a is composed of 3 short stadial events and probably “Heinrich types” events (Palumbo et al., 2013; Voelker et al., 2010) which correspond to detachments of icebergs from Laurentide Ice Sheet and rise toward the North Atlantic (Rodríguez-Tovar et al., 2019).

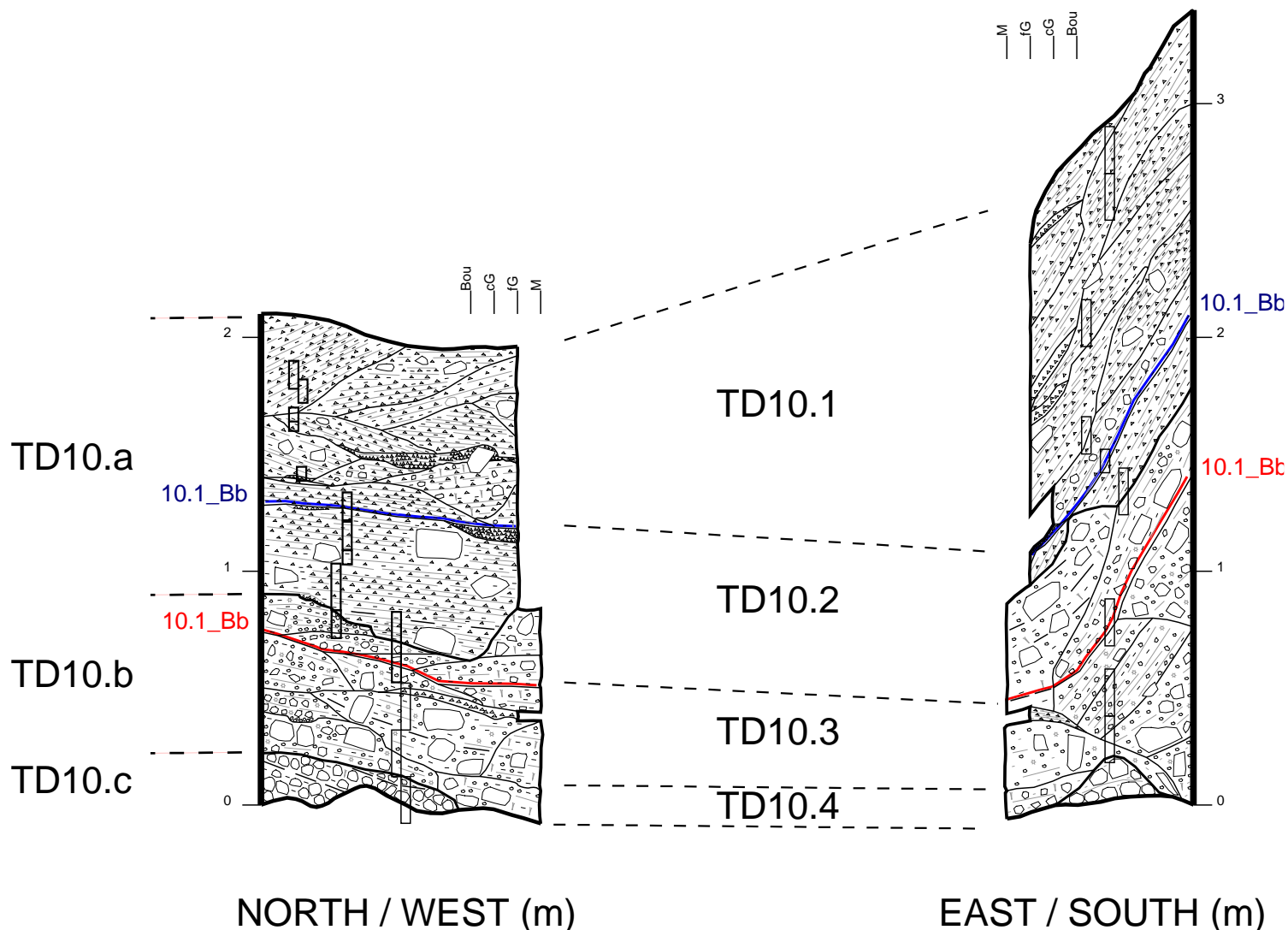
Finally, MIS 9 represents an interglacial period that is considered to be as warm as modern times. (Webb, 2013; Wu et al., 2023). It is divided into five sub-stages, with three warm periods and two cold periods. MIS 9b corresponds to one of these cold periods and is associated with TD-10.1 (Wu et al., 2023).

In some, according to the MIS, TD-10 unit present two cold period, TD-10.4 and TD-10.1 in alternance with one warm phase, TD-10.3 and TD-10.2, according to the MIS.

Gran Dolina TD-10 stratigraphic unit

TD-10 layers can reach three meters thick, and represent the most important middle Pleistocene layer of Gran Dolina (Ortega et al., 2017). This layer presents four subunits, from the bottom to the Top TD-10.4, TD-10.3, TD-10.2 and TD-10.1 (Figure 2)

Figure 3: Stratigraphic units proposed from TD-10 of Gran Dolina site based on field observation-Sinthetic logs from site outcrops with the position of the samples for soil micromorphology and petrographic studies included in this MTh..



Following stratigraphic representation (Figure 3), unit TD10 can be separated into three well-differentiated lithologic units (TD10a_b_c). However, archaeostratigraphic studies distinguish 4 units (TD10-1 to TD10_4) from units based on preliminary work developed in the 90s. The sediments of unit TD10_1 to TD10_3 show common features as they are secondary/illuvial filling of breccias with angular Cretaceous dolomitic rocks of a size around the small boudoir (128 - 256 mm).

The stratification of TD10_1, and the upper part of TD10_2, is a lamination made of very fine to medium mud and gravel (2 to 16 mm). The lamination of the lower part of TD10_2, where TD10_Bone bed, and TD10_3 are included, is coarser and consists of medium to very coarse mud and gravel (8 to 64 mm). The angular character of these breccias indicates that they are related to colluvial rock falls. In order to explain the secondary sedimentary filling and the microstratification / lamination of the sediments in these breccias of TD10_1, TD10_2 and TD10_3, we can refer to their similarity to slope deposits described as ordered scree or screes, formed by runoff or solifluction (debris creep)(Bertran & Texier, 1999; Blikra & Nemeč, 1998; Lenoble, 2005) linked to grain flows.

TD10_4 contains very small boulders (64 - 128 mm) well sorted with variable support matrix to clasts very little stratified. These very fine boulders are subrounded and show a black patina and developed cortex. The matrix is very muddy and forms cracked prisms with blackened faces.

The sorted character of the very fine boulders, their patina and their watering indicate their relationship with resedimented debris-fall deposits. The poorly stratified and very muddy character of the sediment of TD10_4 / TD10 c is related to erosion deposits where the decantation of the mud is put in place in subaquatic conditions, during the fall of the high water current regime (Lenoble, 2005).

Chapter 2: Set of Art

The Sedimentary facies constitute an important part of any stratigraphic studies, in particular inside archaeological research. Thank to them, the archaeologist can understand the environmental/ geographical context of the different sediment deposit that constitutes the sites (Nichols, 2009). In some context, they can provide the only environments data disponible. For example, some sites due to conservation problem presents a lack of faunal and/ or pollinic remain (e.g. oxide condition for pollen). Therefore, the sediment become the only remain of the past environments. Understanding the different sedimentary facies is therefore essential to archaeological sites comprehension.

The literature review of this master thesis has to objective to present the significant information on the previous research conducted on the depositional context and the sedimentary facies of Gran Dolina TD-10 unit which is the focus of this study.

Gran Dolina TD-10 layer

Previous Research on the Geological Depositional Context of TD-10 units

Since its discovery, the stratigraphy of Gran Dolina and the different sedimentary facies which compose it have already been the subject of numerous studies. Those studies have been able to put out the evolution of Gran Dolina cave during the Middle Pleistocene. Indeed, 12 facies have already been observed and describe in all the stratigraphy of Gran Dolina, and can be class into different groups. Gran dolina present so, debris fall facies, debris flow facies, channel facies, mud flow facies, floodplain facies and decantation facies (Campaña et al., 2017).

The TD-10 layer constitutes the moment where the roof of the cave falls apart, creating in consequence the fall of important pieces of the roof block and therefore an increase communication between the outside and inside of the cave. This is why, this layer presents an important proportion of sediment coming from outside the cave. The opening of the roof during the formation of TD-10 units happened progressively and begin during the transition between the TD-9 to TD-10 units. This led to the cave system to change from an endokarstic to an exokarstic compartment (M. Hoyos & Aguirre, 1995). Because of that, the TD-10 layer can be seen as a detrital unit with different subdivisions. This indicates a notable change in the regime and evolution of the cavity, which is entering a new cycle of karstic

activity (Gil et al., 1987). All those changes are reflecting inside the different sedimentary facies, and have been interpreting differently according to the authors. Two main hypotheses explain the formation of TD-10 units. The first one hypothesis associates the TD-10 unit debris flow, but also mud flow and decantation facies which are associated to fluvial environments (Campaña et al., 2017). However, some authors associate the formation of TD-10 units to gelifluction, rock fall deposit and debris flow as part of avalanche (M. Hoyos & Aguirre, 1995).

This two vision of TD-10 oppose two types of deposits : alluvial (fluvial flow) and alluvial deposit (avalanche). The colluvium deposit and process are often confused with alluvial deposits and processes inside the literature. In fact, historically speaking, the term of alluvium and colluvium are linked. Indeed, the term of colluvium was first introduced to designate deposits where it was impossible to tell whether they were alluvium or diluvium (Miller & Juilleret, 2020). This term was also used to designate deposits that were neither alluvium nor diluvium (Emory, 1857; Schott et al., 1854). Before the definition of Kerr (1875), alluvium like with rock fragment bigger than the one finds inside alluvium, the colluvium deposit was not considerate as a sediment category (Miller & Juilleret, 2020). Since then, the term "colluvial" has been used by many authors who have given it their own definition.

Inside this master thesis, we will use the colluvial definition of Blikra (1998). Colluvial processes are so one of the geogenic processes that add new sediment to sites and designate any clastic slope waste material (Blikra & Nemec, 1998). Generally, colluvium are deposits link to gravity process , and are accumulated in the lower part of a slope (Bates & Jackson, 1987; Blikra & Nemec, 1998; Holmes, 1965). Colluvial processes are numerous and correspond to several types of transport and deposition. In fact, Rock fall, debris fall, debris flow, snow flow and water flow are all part of the deposition process and colluvium facies . All these alluvial deposits generally take the form of a fan or cone, which is rather short and steep. (Blikra & Nemec, 1998). On the other hand, an alluvial deposit is defined as : “ (...)Materials deposited on the land surface from transport by flowing water confined to a channel or valley floor” (Eggleton, 2001).

Therefore, colluvial and alluvial deposits present some differences. Firstly, alluvial fans and colluvial fans are not found inside the same geomorphological context. If both of them are associate to slope, alluvial fans are identified in mountains and mountain base, while alluvial fans are located inside the mountain floodplain and valley floor. The types of sediment transport are so different from each deposit. Colluvial present avalanche depositional

processes (e.g. Rock fall, debris flow, snow flow, small water flow in gullies...) while alluvial is the result of debris flow and water flow associates to fluvial context (e.g. braided streams). Secondly, the colluvium fan presents a slope steeper (35-45° at the apex and 15-20° at the toe) than the alluvial fan slope (10-15° at the apex and 1-5 at the toe). Because of that, the surface occupied by the fan is different according if it has a colluvial or alluvial origin. Alluvial fans are more spread out (10 to 100 km) than alluvial fans (0,5 to 1,5 km). The sediment that composes those deposits are also different. The alluvial fan present mostly gravel very immature and alluvial fans can present gravel but also sand which can be immature to mature. (Blikra & Nemec, 1998). Yet, all that information was made on no burial colluvial and alluvial fan, the difference between the two types of deposit can be more difficult once burial and with age. This is why the utilization of other characteristic, like microscopy, to describe the colluvial can be very interesting.

Nonetheless, in the absence of any international convention, the term colluvium remains ambiguous, as it has different meanings depending on the author and the country. This explains why colluvium processes are still often confused (Miller & Juilleret, 2020). For all those reasons, the term of slope deposit could be more adapted for the TD-10 unit description. This broader qualification could help to avoid any confusion that the term colluvial can bring but also expand the possible transport types responsible for the formation of TD-10 and the utilization of microscopic features as criteria of classing. Indeed, the different mass movement, which can form the slope deposit (Blikra & Nemec, 1998) present different microstructures. The rockfall and debris fall can be recognized by the presence of openwork and clast presence showing random orientation. The clasts coming from free fall are angular and unsorted. Some inverse grading can be observed in those deposit due to the dry grain flow (Karkanias & Goldberg, 2018). The solifluction is typical of periglacial environments. These types of deposits are characterized by plates and granular microstructures forming due to the ice presence (Bertran & Texier, 1999; Van Vliet-Lanoë, 2010). Some vesicular crust and capping can be observed at the surface (Karkanias and Goldberg 2019; Harris and Ellis, 1980; **Courty and al, 1994b**). Debris flow presents a fine-grained silty clay matrix more or less homogenous where coarse particle spread inside. They can present vesicles even if there are not characteristic of debris flow (Bertran & Texier, 1999). In addition, those deposit do not present any regular microscopic lamination, grading, or good sorting which are typical of water flow. Rotational features are often meet inside debris flow. The mud flow presents

some porphyric-related distribution with a dense and homogenous matrix presenting a lack of pores with the exception of the vesicles presence (D. Friesem et al., 2011; D. E. Friesem et al., 2014; Gé & Guilloré, 1993; Karkanas & Efstratiou, 2009; Karkanas & Goldberg, 2018) Water flow present lamination of fine-grained sheets wash deposits as characteristic microstructure (Bertran & Texier, 1999; C. A. , Mùcher et al., 2010). The laminations present are moderate to very well differentiated in size. Those laminations can only be horizontal or sub-horizontal (H. J. Mùcher & Vreeken, 1981). Other features can be observed like loose aggregate, free-clay wash, and loose to dense infilling of packed rock and mineral grain or clay-rich aggregates in case of intense rainfall (Karkanas & Goldberg, 2013; H. J. Mùcher & De Ploey, 1977).

The main paper dedicated to slope deposit facies. Once of the most important work on the subject is the paper of Bertran and al (1999). This paper presents the different facies and microfacies of the different slopes deposit, rockfall, streamflow, hypercontracted flow, rock avalanche, debris flow, solifluction and earth slide, both at macroscopic and microscopic scale. Therefore, this paper and its various descriptions provide an excellent comparison for analysing the different deposits on the TD-10 layer by using microscopic characteristic as classing tools, and so, to try to distinguish the deposit context of Gran dolina (fluvial flow VS gravity flow). That is why it is one of the refers papers of this master thesis.

TD-10 units present an interesting alternance of matrices and clast deposit, described by Campaña as debris flow and decantation or mud flow facies. However, simpler hypotheses utilizing a single mode of transportation exist to explain the clast/matrix alternatives, for example, the concept grain flow or grèze lité deposits. Grain flow is a slope deposit processes resulting from a mix of important sediment concentration and air. As the TD-10 is the layer of cave roof fall, the presence of grain flows inside it deposits seem possible (Bertran & Texier, 1999; M. Hoyos & Aguirre, 1995).

The “grèze lité” was firstly defined by Guillen in 1953 as “(...) slope deposit which can be defined as greze, and which present a superposition of beds more or less continuous, thick, homogenous in vertical cut”. Later the term of “lit gras” and “lit maigre” was introduced to differentiate the different bed. The association of one “lit gras” and one “lit mince” successive form a “cyclothème” (Dewolf & Guillien, 1962). It exists different hypotheses which tries to explain the formation of “grèze lité”. Those formation could be the result of

freeze/thaw. The water coming from the ice melt percolated on the rock formation taking debris with it. The difference of the thickness of the different bed, "lit gras" and "lit mince", are so explained by the inequality of water debit (Guillien, 1951). Other hypotheses attributed the formation of "lit gras" by freeze-fluction (congelifluction) and the formation of "lit maigre" by the washing of lit gras superior part and percolation due to liquefaction (Bertran et al., 1992; Journaux, 1976). In this case the percolation plays an important role (Washburn, 1979)

The utilization of the slope deposit, "grèze lité" or grain-flow model imply to change the facies description of TD-10 units. This change could be necessary as some point of TD-10 are not well understood. Indeed, the climate and its variation of TD-10 need more investigation. Certain data attempts to define warm and humid climates and other rather cold climate sometime in the same sub-layer. This is why the description of the facies of TD-10 presented in this literature review seems insufficient to be able to point out the last grey area that this layer of Gran Dolina presents. Therefore, this thesis will take back the analysis of the TD-10 layer specifically to define new facies at a smaller scale, by using micromorphology tools instead of field observation as it was previously made.

Dolina TD-10 Units, Previous Sedimentary Facies Description Research

The most recent description of the TD-10 units facies is the one realized by Campaña and al (2017) and associate TD-10 units with alluvial deposits. He defined three debris flow facies as : "(...) clast support boulder with muddy matrix facies", "(...) matrix supported boulder and gravel with muddy matrix" and "(...) Grain supported boulder" , respectively designate as Facies C, Facies D and Facies F. They present a number of similarities. All three facies contain boulders, but also gravel. Moreover, they do not present any grad and Facies C and D present a low sorting (poorly sorted inside the Facies C and unsorted inside the Facies D). However, if these facies are observed more closely, several significant differences can be noted. First of all, those facies present boulder from different size, small subangular and elongated boulder for the facies C, medium boulder for the facies D and medium to small for Facies F. The concentration of gravel is also different, and only present in low concentration inside the Facies C. To finish, the Facies C and F present massive facies while the Facies D is a chaotic. (Campaña et al., 2017). In addition, to the debris flow decantation

facies and mud flow have been identified. The decantation facies present with a yellowish-red colour due to the presence of clay and silt and very thin horizontal lamination. Contrary to the facies discuss above, no clast or gravel is observed. The contain sand is also very low (<20%). The principal size of the clay is coarse silt. Inside TD-10 units, the decantation facies do not exceed more than 10 cm thick (over 2-3 m). The mud flow facies present inside Gran Dolina, and so in TD-10 units are linked to distal sediment or low energetic flow. Generally, it presents a tabular form (5 to 30 cm thick), with no sorting and fine sediment (around 80% of clay and 20% of sand). It has been observed that this facies are more frequent inside the SE than the NW section (Campaña et al., 2017). We can so give the description of TD-10 as a succession of debris flow coming from the west opening of the cavity and with little input of lateral opening and rock fall even inside a fluvial environment indicated by the presence of small decantation and mud flow facies (Campaña et al., 2017). The repartition of this different facies vary according to the stratigraphy of TD-10. Mud flow facies are found in subunits TD-10.4. This could be the result of a reduction in the size of the inlets (Pares and Perez-Gonzalez, 1999) or a distal position within a debris flow (Campaña et al., 2017). In addition, this subunit has a high percentage of the matrix. This high matrix content could indicate that the soil formed outside the cave-in warm, humid conditions (Blain et al., 2009; Cuenca-Bescos et al., 2005; García-Antón, 1995). Yet, some authors have interpreted this subunit as being the result of a cycle of gelifluxion of the ridge bed and a significant amount of water from melting ice, due to the significant presence of gravel. The deposit would have accumulated before sliding down the slope, with a low velocity and showing little or no internal modification of the primary structure. Within this sub-layer, there would be 3 subunits, 2 of which would correspond to a cold phase separated by a warmer, wetter subunit (little or no winter process) (M. Hoyos & Aguirre, 1995).

Other fluvial event, probably decantation facies are present at the top of TD-10.2, and three other are observed at the bottom, at the middle and at the top of TD-10.1 sub-layer (Campaña et al., 2017). Despite, the sub-layer TD-10.3, TD-10.2 and TD-10.1 present a poor matrix unit and an important presence of debris flow facies (Facies C and Facies F) which could indicate a poor soil formation outside. The reason of it could be due to more cold climate condition as the pollinic and faunal data suggest (García-Anton, 1995 ; Lopez-Antoñanzas et Cuenca-Bescos, 2002), yet, the lack of glacial vertebrate remain seem in contradiction with the presence of glacial climate (Blain et al., 2012; Rodríguez et al., 2011).

The TD-10.3 sub-layer present three subunit (M. Hoyos & Aguirre, 1995), and also at least 3 debris flow facies F event (Campaña et al., 2017). The boulder finds inside this sub-layer correspond to part of the cave roof which falls due to the intern evolution of the cave: the erosion inside (roof) and outside (slope) the cave contributes to thinning the roof of the cave until it collapses. (M. Hoyos & Aguirre, 1995). Those events could have created an enlargement of pre-existing entries or an opening of new entries. A new entry seem compatible with the present of deposits from the SE inside this sub-layer, while the majority of the facies sediment of TD-10 come from the NW section (Campaña et al., 2017).

The TD-10.2 is a subunit of run-off water transport. It does not present or very few channel structures. The opening/ fall of the roof continuous inside this sub-layer probably due to weak intensity gelifluction process. This probably indicates cool climate condition with humidity seasonal variation (P. A. Hoyos & Cortés, 1981) To finish, according to Hoyos et al. (1995), the TD-10.1 is a washing layer, which could indicate a more humid condition.

As mentioned above in this literature review, the description and the interpretation of the unit TD-10 of Gran Dolina presents several challenge, particularly regarding the depositional modes involved and the potential climate variation. As a result, the established descriptions of TD-10 different facies appear insufficient. Therefore, this master thesis take back the analyses of TD-10 facies specifically to define new facies at a smaller scale, by using micromorphology tools instead of field observation as it was previously made.

Chapter 3: Material and method

Thin section preparations:

The samples used in this study are coming from Gran Dolina, Atapuerca (Spain) and have been taken from the Layer TD10 of this site. Those samples are undisturbed sediments of three different columns (N12, N16/N17 and K22). They were extracted using the plaster method due to their friable and loose nature. This extraction is a key step, as any disruption of the vertical continuity present in the samples must be avoided to conserve the stratigraphy of the samples. The orientation of the samples must therefore be marked. (Fitzpatrick, 1984; McBurney, s.d). Pictures have been taken before and after the plastering and extraction to record their position. After their extraction, all the samples have been sent to the units of geoarchaeology laboratory of IPHES in Tarragona (Spain). Each sample taken was labelled according, the name of the site, the years of extraction, the sample outcrop area and grill and the strata sampling (i.e. ATA 22' TD 10/2/N17/1.). The labels of the samples specially collected for this study are summarized in Table 1. The nine sample's plastered, have been open and dry for 5 weeks, in a drying furnace at 20 °C, with the last 48 H heat at 35 °C and a daily monitoring of the sediment drying process (McBurney, s.d). This drying process has been realized thank to an oven Selecta DRY BIG 2,003,741 (Figure 4) equipped with an air supply motor and an extraction motor. This step allows avoiding any moisture formation and extracted all water present inside the porosity of the sample in order to obtain a good impregnation of each block (Fitzpatrick, 1984; McBurney, s.d). Once the samples have been dry, their thickness has been reduced with great care to limit the use of the impregnation resin and obtain a better result.

To impregnate the sample, more than 80 L of polyester resins and 20 L of acetone have been used. To obtain a really efficient resin polymerization and a good impregnation, a rapport of 3:1 resin/acetone combines with 0.004% of a catalyser, the methylethylketine peroxide (MEK), and 0.002% of an accelerator, the cobalt octoate have been used (Fitzpatrick, 1984; McBurney, s.d). The blocks with the impregnation polyester resin were placed for 48 H at 40 atm (400 mb) inside a vacuum chamber (Figure 6) to dry and avoid any fast movements of the air present inside the sample porosity (Jogerius et al, 1975; McBurney, s.d). This equipment is equipped with an air extraction, which traps the air from the vacuum chamber inside an aqueous solution. Once this first step of dryness has been complete the blocks have been put to continuous to dry in a ventilate place for a time of five weeks (McBurney, s.d). It is important to keep changes in temperature and light exposure to a minimum to minimize the risk of cracking in the resin.

When the resins have been solidified, the different blocks were cut with the help of a 500 mm water jet saw (BROT 1.02.04) (Figure 5). The water jet saw is equipped with an articulated air extraction system and a mud decanter to collect the mud and polyester resin mixed to avoid any environmental contamination. The excess of resins was removed and thrown in a special bin for security reasons (McBurney,s.d). The blocks were shaped in a glass size of 14x6x0.2 cm. For each block extracted, several impregnated blocks of the glass size were cut, some to continuous the thin sections preparation and some to archive. It is important to note that a small notch has been realized on each block shape cut and isolated to indicate the top of the block and conserve the orientation indication. (McBurney, s.d).

N16/N17 block column label	Block length (cm)	K22 block columns	Block length (cm)
ATA'22 TD10/2/N17/1	50	ATA'22 TD10/2/K22/1	34
ATA'22 TD10/2/N16/1	20	ATA'22 TD10/2/L22/1	20
ATA'22 TD10/3/N17/1	32	ATA'22 TD10/2/K22/2	20
ATA'22 TD10/3/N16/1	30	ATA'22 TD10/3/K22/1	30
ATA'22 TD10/4/N16/1	24		

Table 1 Labelled monoliths extracted from unit TD 10 in Gran Dolina, Atapuerca (Spain), years 2022 and their length associated



Figure 4: Drying Furnace



Figure 5: Water Jet Saw



Figure 6: Vacuum Chamber

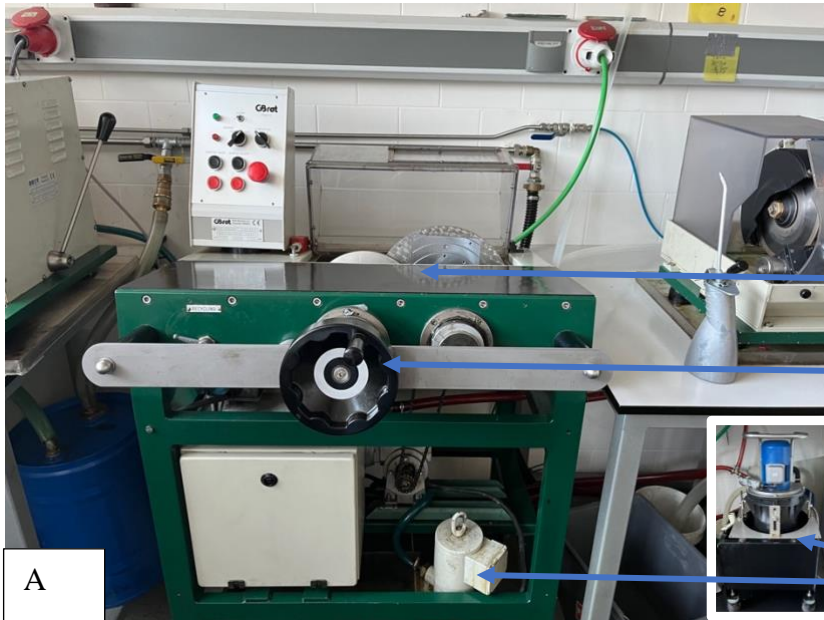
The impregnated blocks, cut in the good dimension, were glued with epoxy resin to a 14x6x0.2 cm temporary glass inside large fume hood (BORDINOLA V21 SPACE ST2100) (McBurney, s.d). The epoxy has been realized thank to resina EC-232 and W-232 in a ratio of 10:2. The block and the temporary glass were let to dry underweight to avoid any deformation of the block (McBurney, s.d)

During that time, the final glasses were prepared. For that purpose, lines were drawn on glasses to serve as markers during the polishing. The final glasses were polished until the line disappears plus five minutes more to obtain exactly the same plane on each glass. The polishing was made thanks to a multiple grinder for 3 samples of size 14x6x0,2 cm (BROT 1 03 12P) (Figure 8.A), equipped with a polishing disc of a bronze alloy and synthetic diamond spikes with a grain size of 30 microns (Figure 8.B). The grinding machine has been decimicrometric feed on a rotary (Figure 8 A) to have a better control of the thickness of the sample its polishing. Cooled paraffin oil (BROT RS5) have been used during the polishing for lubrication. The multi-plate grinding machine is also used to grind the block glue to the temporary glass following the same step of preparation (line draw, polished...) (Figure 8.B). This allows us to have the same plane surface between the final glass and the impregnated block. The polished blocks are then degreased from the paraffin oil using to no toxic hydrocarbons in a large extraction hood (McBurney, s.d). The final glasses and the polishing blocks were glued together inside a large fume hood. The glue between the block surface and the final glass is realized with epoxy resin using a bounding unit (BROT 1 04 04) heated to 40 ° C (Figure 7) during 24h to avoid any air bubble formation and deformation inside the thin section (McBurney, s.d).



Figure 7: Bounding units (Photo-Opeyemi Adewumi, 2019)

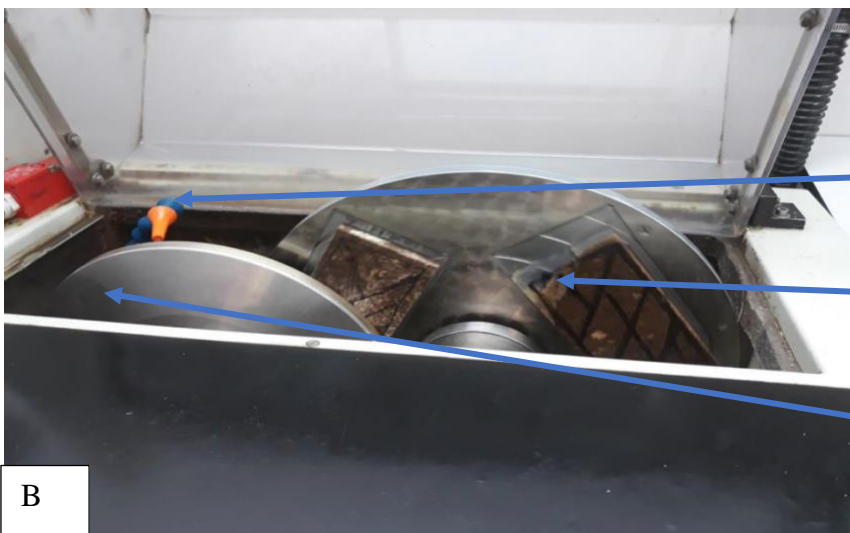
Figure 8: Multiple Grinder Machine with A) General view of the multiples grinder machine, B) Grinder system



Grinding disc for 3 samples

Decimimetric rotary system

the dirty oil is collected (on the left) before to passes through a filter system (on the right) and being re-injected into the circuit (closed circuit).



Jet of cooled parafine oil for lubrication purpose

Sample with line draw as a marker for the polishing process

Polising disc made of bronze alloy and diamond spike

To finish the thin sections were clean with Quina paraffin to remove any oil and dust before to be covered with thin glass protection with resin (Figure 9). Cover the samples allow a better conservation and observation in a petrographic microscope, but prevents the possibility of chemical analysis.

All the impregnation and thin section preparation processes were carried out in accordance with the method developed by Guilloré (1980) and Mcburney (s.d).



Figure 9: Final Thin section of a thickness of 30 micron (Photo-Opeyemi Adewumi, 2019)

Thin section observation and description

The thin sections have been observed thank to a ZEISS (AXIO scope) microscope with object x10, x20, x50, x100 and x 200 in normal polarized transmit light, and normal incident light as well as with an OLYMPUS (BHSP 203976) microscope with the objective x10, x40, x100, x200 in normal polarized transmit light and normal incident light. The main difference between those microscopes is that the OLYMPUS microscope is equipped with two sets of two ocular and so allow two monitors in the same time. This microscope was mostly used, during the discussion. Moreover, all the thin sections were scanned thank to an EPSON V500 PHOTO and picture of the microstructure and pedofeatures have been obtained with a DELTAPIX invent 5 S digital cameras mounted on the ZEISS Axio Scope. All those different equipments have allowed us to observe the thin section at different scales, to identify the different elements, mostly microscopic structure, inside the thin section. Both microscopes were used for the observation and description. The scanner was used to obtain a global vision of thin sections and the observation of some feature, like the class distribution, porosity, aggregate... which are

better observe in that mode. To finish the camera has enabled us to take precise picture of microstructure present inside thin sections.

In addition to the thin sections prepare by ourselves, thin sections already made and coming from the same columns (N12-N16/N17 and K22) have been included in the description and discussion of this study. In total, 43 thin sections have been analysed, for a total of 28 block extracted from the site (19 from 2010 and 9 from 2022). The thin sections are named according to the label of their block and their position inside the block, superior (sup), medium (med) and inferior (inf). The labels of each thin section are resumed inside the Table 2

To obtain a better and efficacy observation on the microscope, thin sections were first organized in microfacies thank to macro-observation in accordance with the macro-feature observes like the fabric, the grading, the sorting and the sphericity. This step allows specially to observe the clasts and pebbles present inside the thin section. After that, microfacies obtains by macro-observation have been quickly analyze under a microscope to first determine their granulometries according to trigon showing the size particle distribution (Blott et all, 2012) as well as the sorting for the microfacies composes of clay, silt and sand (Bullock et all, 1985). The combination of all those observations give the texture of each microfacies.

Thin section name	Columns	Thin section number	Stratigraphy level (cm)
ATA'10 TD10 K22-1 Sup, Inf	K22	1	TD 10 SOUTH EST -14
ATA'10 TD10 K22-2	K22	2	TD 10 SOUTH EST -34
ATA' 10 TD10 K22-3 Sup, Inf	K22	3	TD 10 SOUTH EST -54
ATA' 10 TD10 K22-4, Sup, Inf	K22	4	TD 10 SOUTH EST -80
ATA'10 TD10 K22-5	K22	5	TD 10 SOUTH EST -106
ATA 10 'TD10 K22-6	K22	6	TD 10 SOUTH EST -116
ATA' 10 TD10 K22-7 Sup, Inf	K22	7	TD 10 SOUTH EST -148
ATA'22 TD10/2/K22/1, Sup, Inf	K22	7 (22)	TD 10 SOUTH EST -114
ATA'22 TD10/2/L22/1	K22	8	TD 10 SOUTH EST -166
ATA'22 TD10/2/K22/2, Sup, Med, Inf	K22	9	
ATA'22 TD10/3/K22/1, Sup, Inf	K22	10	TD 10 SOUTH EST -186
ATA'10 TD10 N12 1 Sup	N12	1	TD 10 NORTH EST -10
ATA'10 TD10 N12 2	N12	2	TD 10 NORTH EST -18
ATA'10 TD10 N12 3	N12	3	TD 10 NORTH EST -38
ATA'10 TD10 N12 4	N12	4	TD 10 NORTH EST -46
ATA'10 TD10 N12 5	N12	5	TD 10 NORTH EST -56
ATA'10 TD10 N12 6	N12	6	TD 10 NORTH EST -66
ATA'10 TD10 N12 7	N12	7	TD 10 NORTH EST -76
TA'10 TD10 N12 8 Sup, Inf	N12	8	TD 10 NORTH EST -92
ATA'10 TD10 N12 9	N12	9	TD 10 NORTH EST -110
ATA'10 TD10 N12 10	N12	10	TD 10 NORTH EST -124
ATA'10 TD10 N12 11 Inf	N12	11	TD 10 NORTH EST -136
ATA'10 TD10 N12 12 Sup	N12	12	TD 10 NORTH EST -156
ATA'22 TD10/2/N17/1 Sup, Med, Inf	N17	1(22)	TD 10 NORTH EST -132
ATA'22 TD10/2/N16/1 Sup, Inf	N16	2(22)	TD 10 NORTH EST -190
ATA'22 TD10/3/N17/1 Sup, Inf	N17	3(22)	TD 10 NORTH EST -220
ATA'22 TD10/3/N16/1 Sup, Inf	N16	4(22)	TD 10 NORTH EST -252
ATA'22 TD10/4/N16/1 Sup, Inf	N16	5(22)	TD 10 NORTH EST -278

Table 2: Thin section labelled used in this study, their numbers associated and with their stratigraphic level

Following this step, all the thin sections, microfacies by microfacies have been observed deeply into the microscope to determine precisely the microscopic features present inside. This step permits the grouping of the microfacies, established on macro-observation, according to the microscopic features that they share and so give the final microfacies and final microstratigraphy. Due to the determination and definition of the microfacies, the different macro-units, link to the different sedimentary process can then be identified thank to reference studies which link some microstructure or pedofeatures to some type of deposit. In this study, the main reference papers used are the paper of Bertran and all (1999, 1997).

In a second point, the microfacies obtains previously have been studied to determine the types of soil. Inside each microfacies from the microstratigraphy established by ourselves, the groundmass (coarse and fine section limit and ratio), the coarse material (fragment of rock and main mineral, carbonate, silicate, ferromagnesium), the fine material (types, and factor of influence of the b fabric), the microstructure and the edaphic trait were analysed thank a petrographic microscope. The description obtain by those observations were then used to establish the type(s) of soil(s) formation and the evolution of the pot-deposition deformation. This sequence can then be put in relation with palaeoclimate data, by using the microscopes features observed as markers of palaeoclimate condition and change. They analysed gave so information about the palaeoclimate of the unit TD 10.

All the terminology used for description are based on the one Bullock et all (1985), Stoops (2003 and 2010), Bertran et all (1999 and 1997).

Chapter 4 : Result

4.1 General Characteristic of the facies and microfacies.

Inside the TD 10 layer, 3 facies, have been identified.

In general, all the samples are poorly sorted with fine to very fine sub-angular to angular gravel and an unordered to weakly preferred orientation fabric.

The ratio between the coarse and the fine material vary and present some geyuric to monic distribution which are mostly porphyric to eunaulic . The fine material presents also two colours common to all the samples, red and brown to yellow/brown with cloudy and dotted limpidity and a first order attenuated colour interference. The b-fabrics of the layer TD-10 are mostly undifferentiated to crystallites.

In addition, some textural pedofeatures were observed in all the samples. Indeed, continuous silty clay coating around grain (Figure 10.1); dusty clay hypocoating (Figure 10.2); equigranular xenotopic crystal intergrowth with low birefringence and brownish colours (Figure 10.3); Pure amorphous cryptocrystalline continuous coating juxtaposed to dusty clay hypocoating (figure 10.4) and Equigranular xenotopic fabric superimposed on complete and dense infilling with juxtaposed sparitic coating (Figure 10.5) The common microstructures to the samples are compound void packing (Figure 10.1), planar void (Figure 10.1) and vesicles (Figure 11.3)

4.2 CLASSIFICATION OF THE FACIES

4.2.1 Rhythmic very fine gravelly mud or muddy very fine gravel lamina sets (Facies 1):

Description:

We can observe rhythmic very fine mud or muddy very gravel lamina-set inside the samples 1 to 10 (include) of the column N12, the superior part of the sample 1 of the column N16/N17 and to finish the first 3 samples of the column K22.

In general this facies is characterized by the presence of inverse grading.

The coarse and fine material

These facies present a ratio of coarse material/ fine material (C/F) of 3:7 to 2:8. The component of the coarse and fine material vary in function of the type of support.

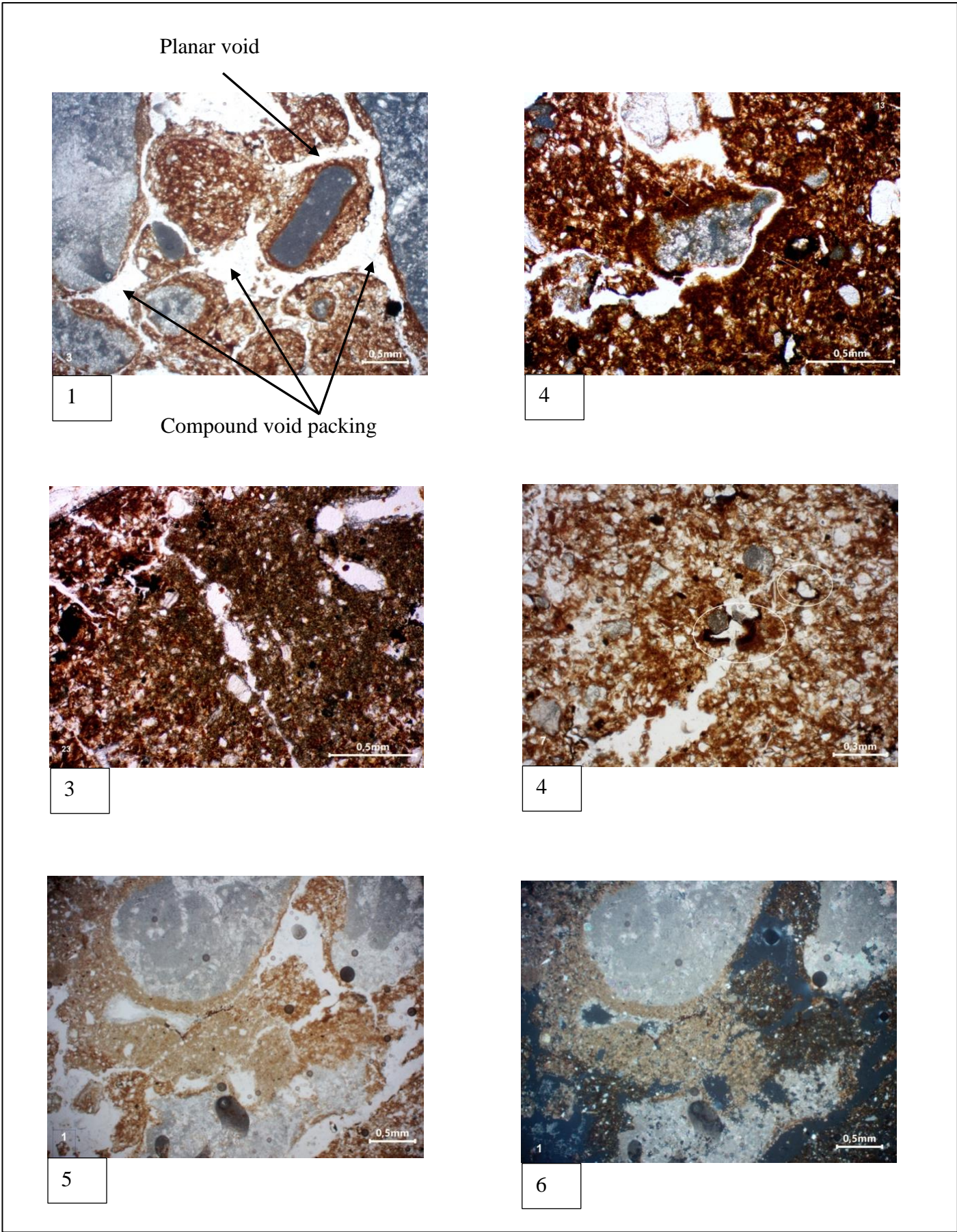


Figure 10: Photography of pedofeatures

- 1) silty clay coating around grain; 2) dusty clay hypocoating; 3) equigranular xenotopic crystal intergrowth with low refringence and brownish colours; 4) Pure amorphous cryptocrystalline continuous coating juxtaposate to dusty clay hypocoating ; 5) and Equigranular xenotopic fabric superimposed on complete and dense infilling with juxtaposed sparitic coating coating

Three types of support were found inside these facies, Openwork to Clast support, Openwork to Matrix support and Matrix to Openwork support (Annexe 1, Figure 1).

The composition of the coarse material varies from very few carbonate (2-5%), very few carbonate silicates (2-5%) and no Ferromagnesium inside the coarse to medium sand fraction to few to common carbonate and silicate (10-20%) and few to very few ferromagnesium (2/5-10%) inside the fine sand to coarse silt fraction inside the Open work to clasts support macro-unit. The two other sub-facies present inside this facies (Openwork to Matrix support and Matrix to Openwork support) the composition of the coarse material varies from very few carbonate (2%), and no silicate and ferromagnesium to very few to few carbonate (2-5%), few silicates and ferromagnesium (5%) inside the fine sand to coarse silt fractions.

The Microstructures and pedofeatures

Three types of microstructure have been described inside each type of support: Crumb, Granular, and Sub-granular. For each type of support and microstructures one Halotype was defined (Figure 11). Along with them, the microstructure granular is the most important one, and is present inside in 24 of N12 microfacies, 4 of N16/N17 microfacies and 9 of K22 microfacies (Annexe 1, Figure 1).

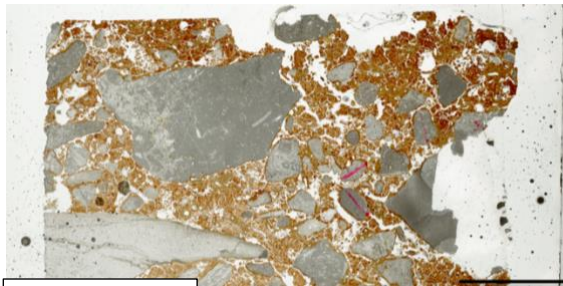
In addition to these main microstructures some channel microstructure have been noticed inside the microfacies N12 XVI, XVIII.

The porosities which have been identified are vugs, channels and simple and complex packing.

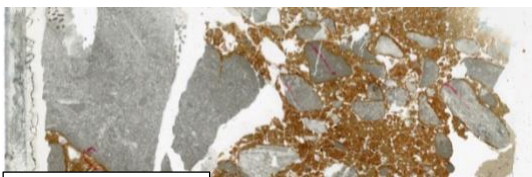
The observable impregnative pedofeatures are crystal, amorphous cryptocrystalline and silty clay hypocoating (Figure 12.1, 12.2 and 12.3) and intercalation, rotational structure (Figures 12.4 and 12.5). On the other hand, the textural pedofeatures are, discontinuous layered sorted silty clay capping (Figure 12.6); inverse graded capping around grain and silty clay aggregate (Figure 12.7); ; dusty clay coating (Figure 10.2); very few discontinuous horizontal micro-layered vesicular crust (Figure 12.8); spirititic coating (Figure 12.9); discontinuous and loose microsparitic and complex packing (Figure 12.10 and 12.11); complete and dense spirititic infilling (Figure 12.12); gelfuric to monic infilling (Figure 12.13); some crystal intergrowth like microsparitic crystal intergrowth and crystal intergrowth with basic orientation referred to channel (Figure 12.14) and discontinuous and loose infilling superimposed to crystal intergrowth (Figure 12.15). and to finish silty clay coating superimposed by crystal intergrowth (Figure 12.16)

Figure 11: Halotypes of the facies 1:

- A) Openwork to clast support; B) Openwork to matrix support; C) Matrix to openwork support
1) Crumb; 2) Granular; 3) Sub-granular



1 (N12 I)



2 (N12 XX)

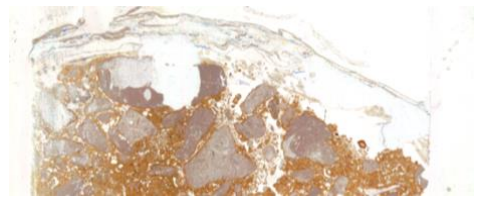


3 (N12 VII)

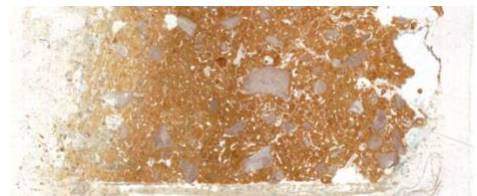
Vesicles



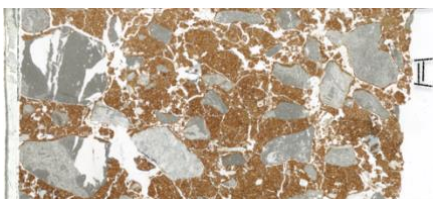
3 (N12 XV)



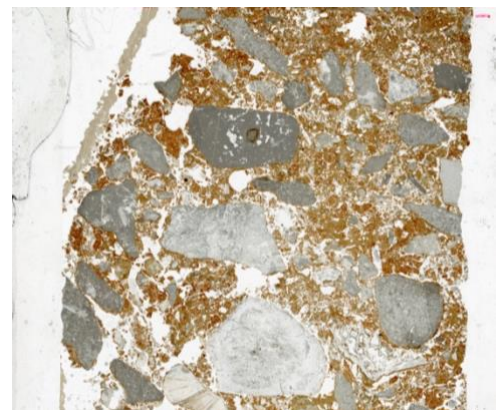
1 (N12 XI)



2 (N12 XIV)



2 (N16/N17 II)



1 (N12 XXXIV)

Interpretation:

Mode of transport and deposit

The granular microstructure can be the result of different activities, Biological, Frost, Colluvial, and due to the rubification process. Inside these facies and microfacies the granule mostly present random coarse material fabric, no association to plates or lentils which these granular microstructures are probably to colluvial or rubification activities (Bertran & Texier, 1999; Mentzer, 2014; Stoops George et al., 2010; Van Vliet-Lanoë, 2010). The presence of continuous silty clay coating around grain, which is typical of alluvial deposits and of turbulent flow of secondary illuviation when it not show layered (Fedoroff et al., 2010; Goldberg & Macphail, 2006; Kühn et al., 2010; Miedema, 2002; Muecher, 1974), seem to indicate a colluvial process. To be more precise the presence of many inverse grading in crudely stratification and an porphyric coarse/fine related distribution with a crystallitic b-fabric seem to indicate a grain flow mode of deposit (Bertran & Texier, 1999). In this hypothesis, the Openwork to clasts support part find in the different thin section regrouped into the facies 1 represent what Bertran and Texier call the top of the sole layer and the matrix to openwork/ Openwork to matrix support part of the basal sole layer of a grain flow deposit. The associate of both types layer than form one grain-flow event (Bertran & Texier, 1999). However, the succession of inverse grading forming the three types of support, the openwork to clast support forming the top of the grad and the Openwork to Matrix/ Matrix to Openwork to basal part of the grad, can also be explained by the concept of “grèze litée”. Inside this facies, who can find some part rich in gravel (coarse material) and some part which are muddier (fine material) in more or less succession. So, it corresponds to “lit maigre” (poor in matrix) and “lit gras” (rich in matrix) (Dewolf & Guillien, 1962) In this case, this facies most be associate to cold climate (°°).

Microstructure and Pedofeatures

Several other pedofeature link to cold climate or frost action were found inside this facies. For example, the different types of capping (inverse and microlayered) were commonly found. Generally, the presence of capping indicates some freeze-thaw cycle sequences. The cap is then organized in two parts: a base made up of fine particles and a skeletane made up of all the coarse particles that have been expelled from the base by the freeze/thaw cycles. It results in an inverse graded capping (Van Vliet-Lanoë, 1987). Inside these facies, most of the cappings do not present any skeletane. We can emit two hypotheses, firstly, it is possible that the number of freeze/thaw cycles was not enough to expelled any coarse material present inside the capping. The other hypothesis is that taphonomical transformation has washed away the skeletane of the capping. It could explain why, some microfacies present inverse capping and/or gefuric to monic infilling. In all the hypotheses discuss above, the

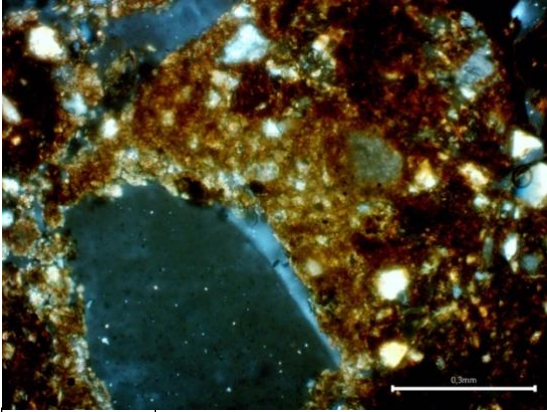
granular microstructure should be the result of frost action (Stoops George et al., 2010; Van Vliet-Lanoe, 2010)

On the other hand, these facies present a lot of carbonates in infilling form. The granular microstructure could then be the result of a dissolution and the recrystallization of the carbonate would then have led to the deformation of the groundmass into a granular microstructure juxtaposed with carbonate granules in the form of infilling. However, this phenomenon appears at only high temperature (Mentzer, 2014). Few granules present cluster of coarse material fabric, which are typical of the biological activities. The presence of channel microstructures is also coherent with the presence of biological activities, like root and animal passage and a surface soil (Stoops George et al., 2010). The crumbs microstructure can also be an indicator of the soil surface, especially of mollisols and verticals, inside this facies (Adderley et al., 2010; Gerasimova & Lebedeva-Verba, 2010; Kovda & Mermut, 2010)(**Kovda & Mermut, 2010a**). Sub-angular microstructure can also be an indicator of surface soil (**Kovda & Mermut, 2010b**), even if this microstructure type is not typical of any types of soil and can also be an artefact of the drying process, or the result of frost action. (Stoops George et al., 2010). The latter seems possible, given the presence of other pedofeatures linked to the frost action. The presence of dusty clay hypocoating can be attributed to a clay accumulation as the presence of dusty clay hypocoating juxtaposed to pure amorphous black cryptocrystalline coating indicates a bad drainage possible of the soil. The explanation of dusty clay coating is still debated. For long times those types of coating were simply interpreted as clay coatings that would simply have aged (Bronger, 1969). However, the discovery of these coatings in young soils calls into question this explanation (Kuhn, 2003).

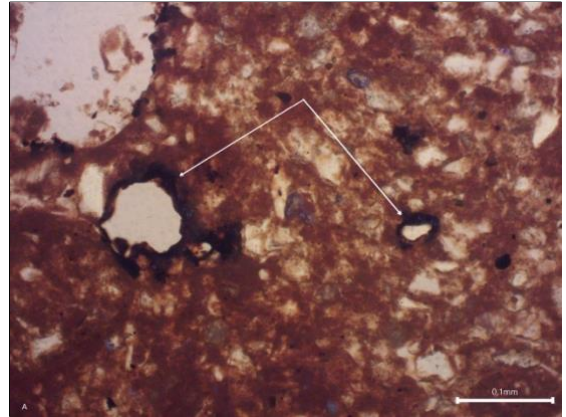
Concerning the microsparitic, its infilling form like all the carbonate infilling is common in arid climate (Stoops George et al., 2010). Its coating and hypocoating form are mostly the result of soil solution percolation on pores or fissure (Courty & Fedoroff, 1985; Kemp, 1995; Sehgal & Stoops, 1972).

Soil determination

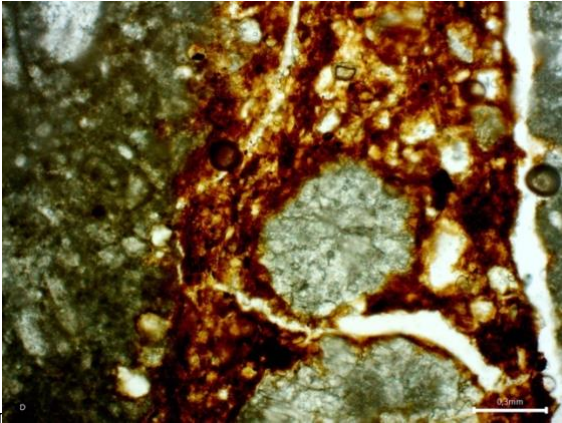
The absence of relict features (e.g. peat), the important presence of granular peds and weathered minerals seem to indicate that this facies is mostly composed of Mollisol or Vertisol, which would have undergone freeze/thaw cycles but not sufficiently or not intensely enough to transform this soil into gelisol (Retallack, 2001), but enough to create frost pedofeature related.



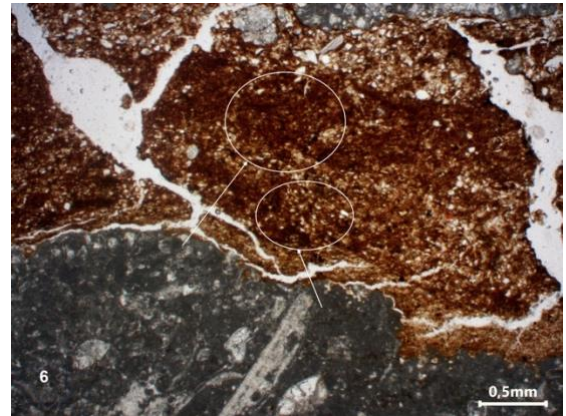
1 (XPL)



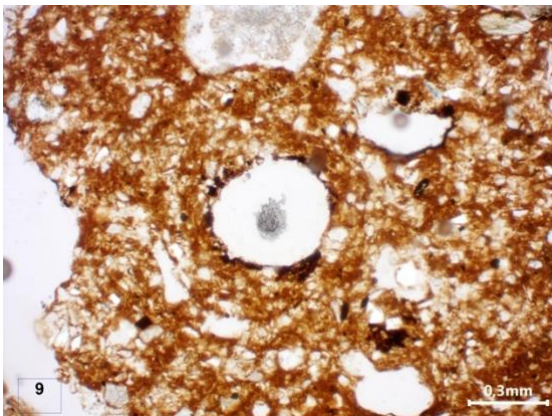
2



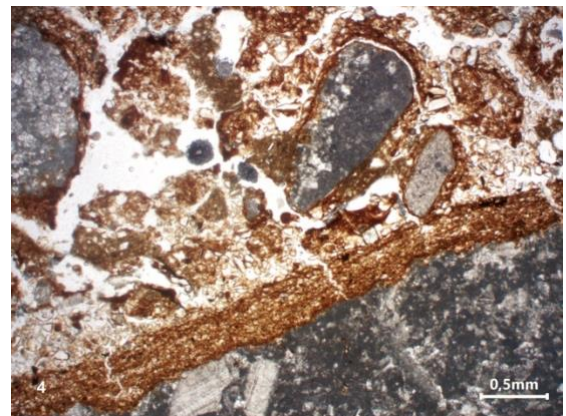
3



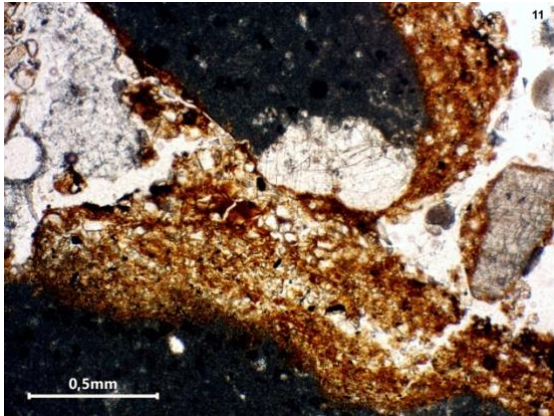
4



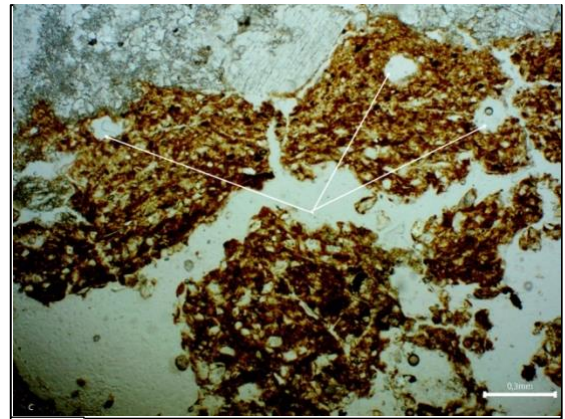
5



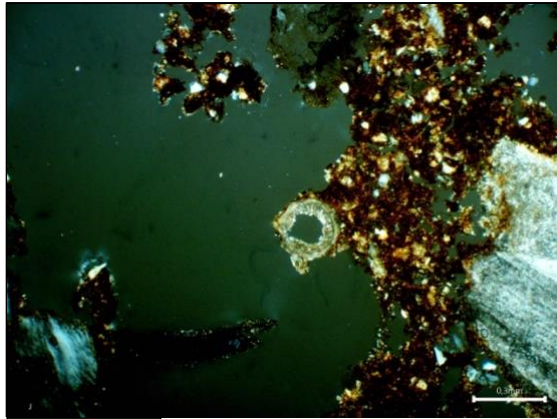
6



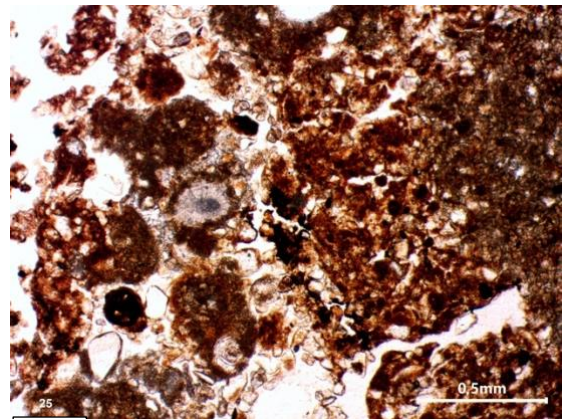
7



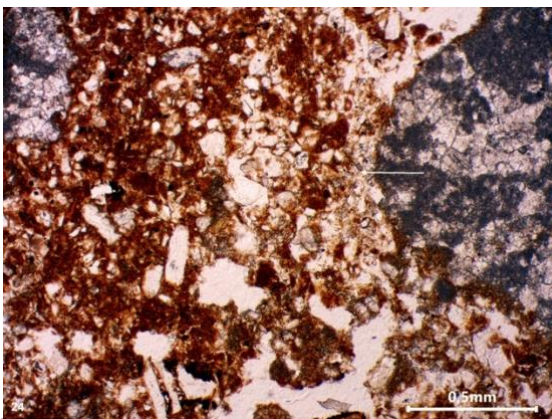
8



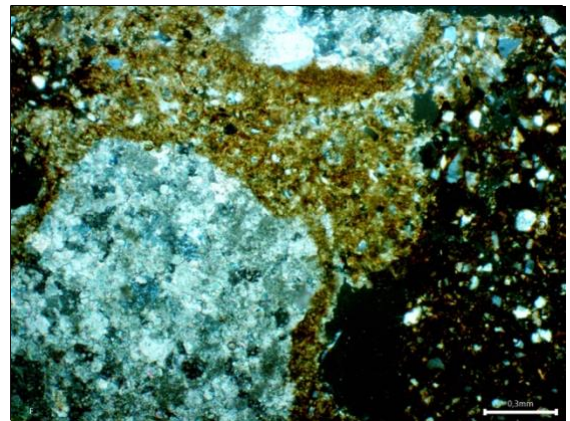
9 (XPL)



10



11



12 (XPL)

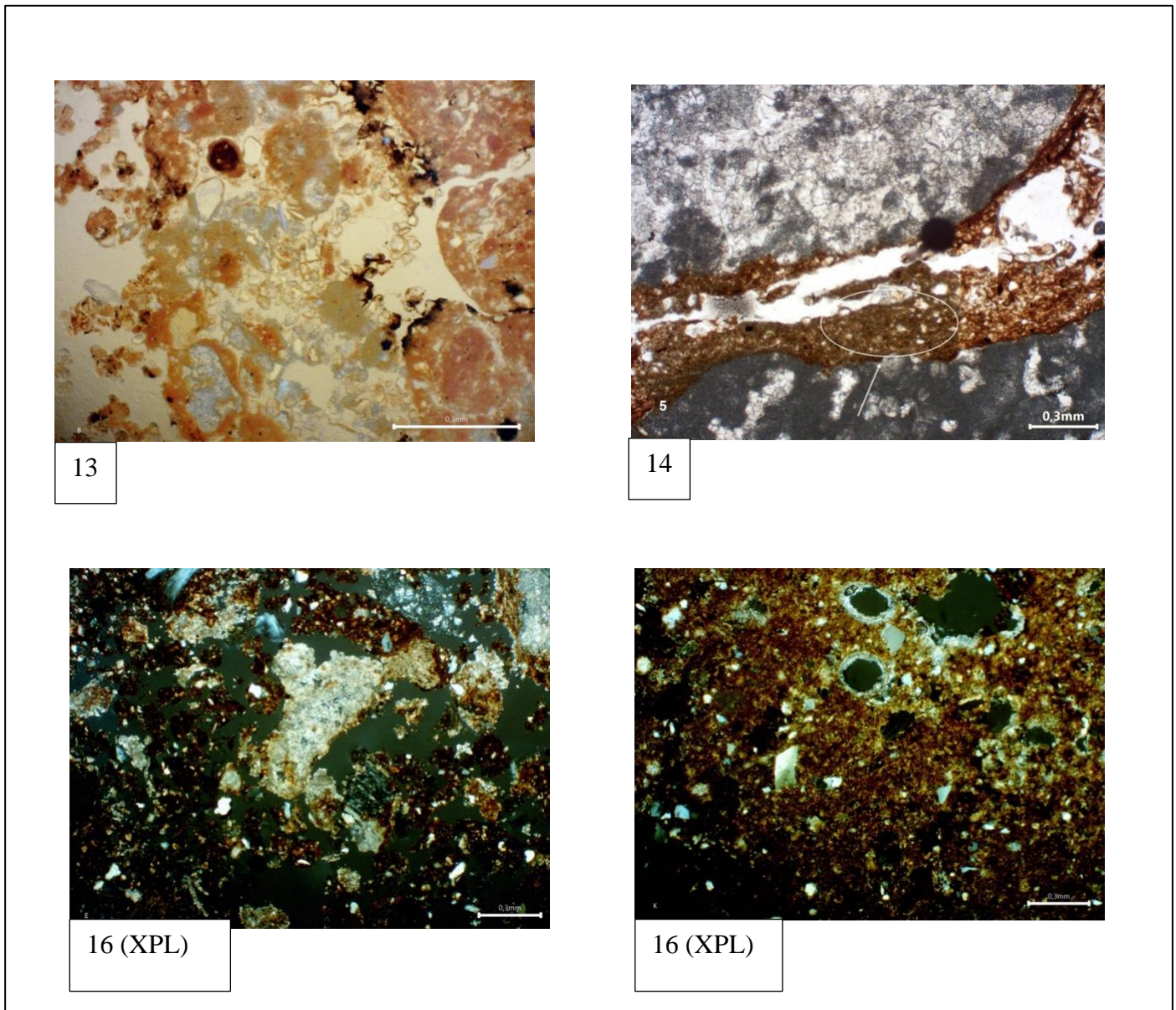


Figure 12: Photography of pedofeatures 2

1) crystal hypocoating: 2) amorphous cryptocrystalline hypocoating: 3) silty clay hypocoating ; 4) Intercalation; 5) Rotational structure; 6) discontinue layered sorted silty clay capping; 7) inverse graded capping around grain and silty clay aggregate; 8) very few discontinuous horizontal micro-layered vesicular crust; 9) spiritic coating; 10) discontinuous and loose microsparitic; 11) discontinuous and loose complexe packing; 12) complete and dense spiritic infilling; 13) gefuric to monic infilling; 14) some crystal intergrowth like microsparitic crystal intergrowth and crystal intergrowth with basic orientation referred to channel; 15) discontinuous and loose infilling superimposed to crystal intergrowth; 16) silty clay coating superimposed by crystal intergrowth

4.2.2 Rhythmic sandy mud to fine gravelly mud in fine besets (Facies 2)

Description:

Those kind of bet-sets are observed inside samples 1 (medium and inferior part), to 4 (included) of the column N16/N17, and the samples 5 (inferior part) to 7 22 (superior part) and 7 13 to 10 (include) of the columns K22.

The coarse and fine material

This facies is characterized by the presence of inverse grading, like the facies 1, but also the presence of some crudely stratification which are not observed in the facies 1.

These facies present a ratio coarse/ fine material which varies from 3:7 to 2:8 and 1:9 to 2:8. The b-fabric present inside are reticulated and parallel striated b-fabric.

The composition of the coarse material of these facies varies according to the type of support and microfacies. The variable support (matrix to openwork support) compose of granular microstructures (Figure 13) is composed of few to common carbonate (20%), few to very few silicates (5-10%) and very few ferromagnesium (<5%) inside the coarse to medium sand fractions and very few to few carbonate and silicates (5-10%) and no ferromagnesium inside the fraction fine to coarse silt.

The Variables support granular to plates microstructure (Figure 13, figure 18) is composed of few carbonate (5%) and silicate (5-10%) and no ferromagnesium inside the coarse to medium sand fractions and few carbonate (5-10%), few to common silicates (20%) and to finish very few ferromagnesium (<5%) inside the fine to coarse silt material.

The part Matrix support presenting plates microstructure (Figure 13) present a variation of the composition of coarse material. The part without diamicton (Figure 18) is composed of few carbonate (5-10%), few to very few silicates (2-5%) and no ferromagnesium inside the coarse to medium sand fractions and few carbonate (5-10%), few to common silicate (10-20%) and very few to no ferromagnesium (<5%). On the other hand, the part presenting diamicton (Figure 18) is composed of few silicates (5%) and no carbonate and ferromagnesium inside the coarse to medium sand fractions. It is composed of few to very few carbonate (5-10%), few to common silicate (10-20%) and very few to no ferromagnesium (<5%) inside the fine sand to coarse silt fractions.

To finish the variable support (Matrix to clast support) with granular microstructure (Figure 13,) (figure 18, K22 columns) is composed of few carbonate (5-10%), and no silicate and ferromagnesium inside the coarse to fine sand fractions and, no carbonate, few to common silicate (10-20%) and few to very few ferromagnesium (2-5%) inside the fine sand to coarse silt fractions.

Along the microscopic features, plate microstructures is the most important one, and is present into most of the N16/N17 columns (microfacies VII to XIII included) and a small part of K22 (microfacies L to LII included) (Annexe 1, Figure 1)..

Microstructures and pedofeatures

The porosities identified forming the microstructures are few complex and simple void packing, few channels and some vughs.

Concerning the pedofeature present inside this facies, we can have observed a lot of pedofeatures links to the frost action like the different capping (microlayered and invers graded), already observed but also some link capping (Figure 14). It also presents some intercalation (complex and simples) and rotational structures. This facies is also full of loose and discontinues microaggregates infilling as well as monic to gefuric infilling. There are also some silty clay hypocoating and pseudomorphic cristallitic coating.

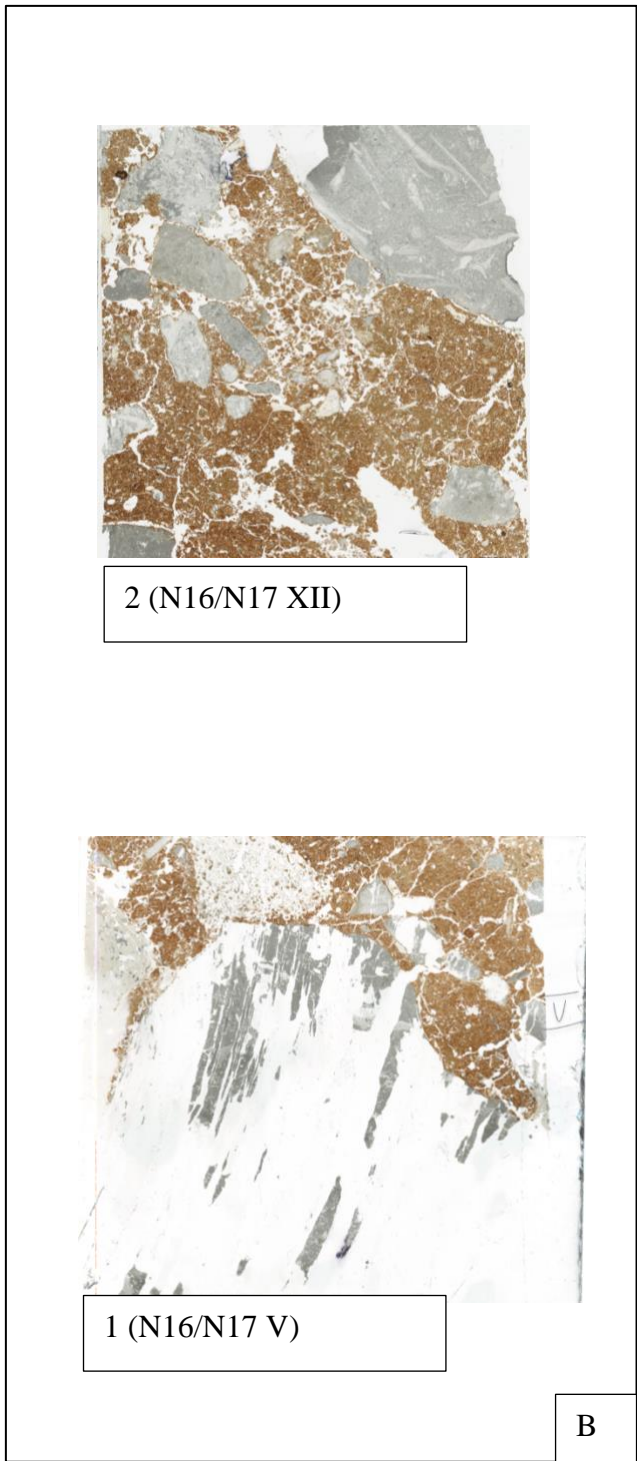
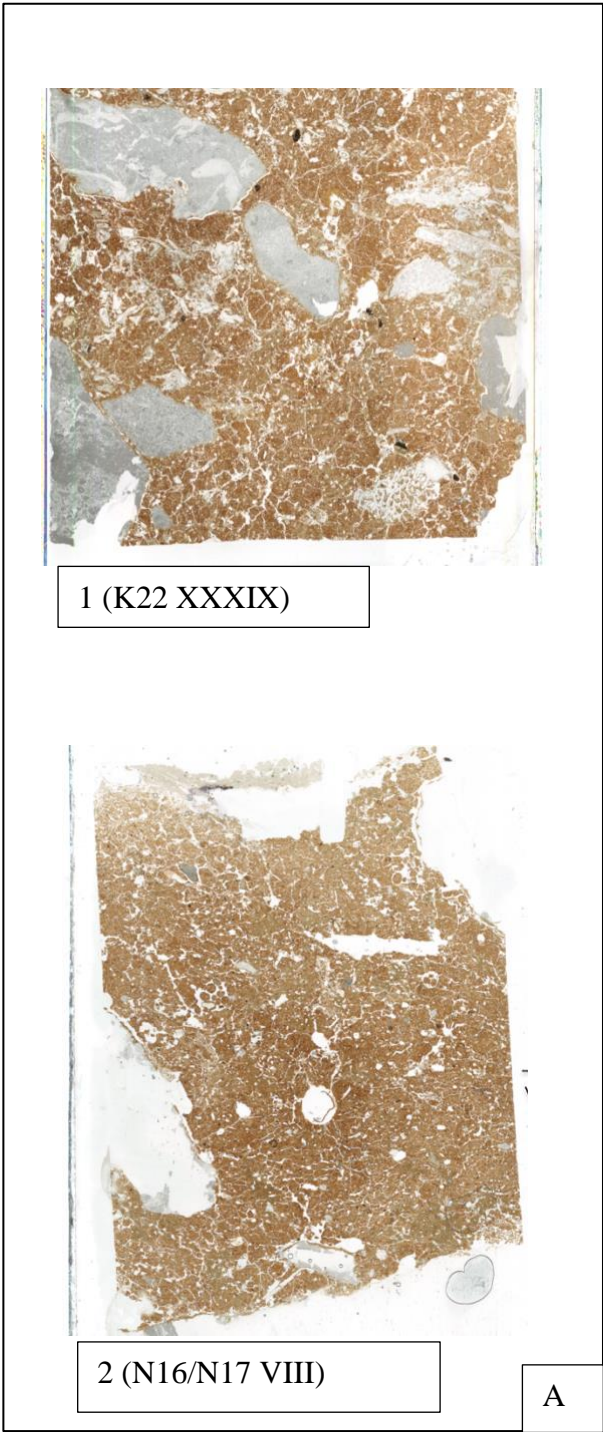


Figure 13: Halotypes of Facies 2

- A) Matrix support
- B) Variable support
- 1) Granular
- 2) Plates

Interpretation

Mode of transport and deposit

The presence of crudely stratified diamicton and the alternance of diamictic and openwork (dark green microfacies altering with dark brown microfacies) present inside the columns N16/N7 are typically the lithofacies associate with solifluction deposit process as well as the plates microstructures. (Bertran & Texier, 1999). However, the absence of plates inside the microfacies K22 XXXVII to XLIX, seems to suggest that solifluction is probably not the only mode of deposition for this facies. It is more likely that solifluction is a deposit mode superimposed on a previous transport and deposit mode.

The presence of the crudely stratification, diamiction, porphyric relative distribution of the coarse/ fine material as well as the undifferentiated or crystallitic b-fabric are also compatible with debris flow. The important presence of boulder, with variable support texture (clast to matrix support) inside the microfacies K22 XLII to XLIX and N12 XXXVIII to XLI is, however, compatible with rock avalanche (Hsü, 1975; Melosh, 1987).

We have so hypothesis that, the facies 2 was created by debris flow process, with possibly some small rock fall inside the microfacies cite above, in which some solifluction has occurred inside the microfacies N16/N17 V to XIII and K22 L to LII.

Microstructures and pedofeatures

The plates microstructures associate to the granular microstructures are typical of frost action (Van Vliet-Lanoe, 2010). The void like planar or vughs are also often associated with those microstructures in case of frost action, as it is the case for the capping present inside these facies. (Van Vliet-Lanoe, 2010). Inside this facies appears, the link capping, which can explain the appearance of b-fabric (reticulated and parallel b-fabric). Besides, the vughs porosities are often associated to frost action or ancient granular soil which have been thought some compaction process. (Stoops George et al., 2010; Van Vliet-Lanoe, 2010). Both possible seem compatible with these facies (As TD 10 is buried under TD 11, which represent several m).

We have also identified some intercalation as well as rotational structures. Those pedofeatures are typically in situ formed (Stoops George et al., 2010). Moreover, clay intercalations have been associated to waterlogging (Fedoroff & Courty, 1987). The rotational structures are also creating in presence of water. Their presence has been documented in case of subglacial diamicton (Khatwa & Tulaczyk, 2001; Menzies, 1998, 2000; van der Meer, 1993, 1997) and debris flow (Lachniet et al., 1999, 2001). In the case of diamicton presence, the rotational structures are formed in a transitory turbulent movement around the diamicton (Phillips, 2006). It is mostly possible that the rotational

structures present there are the result of subglacial diamicton as the plates suggest a cold climate and several diamictons have been found in these facies (microfacies N12 XXXVIII; XXXIX; XL; XLI; N16/N17 VIII; IX; X; XII; XIII and K22 XXXVII; XXXVIII; XXXIX; XL; XLI; L; LI; LII).

With all these elements, we can deduce that most of the granular microstructure present are the result of frost action.

The silty clay hypocoating present diffuse boundary and a composition close to the groundmass, which indicate an in situ formation. (Stoops George et al., 2010).

The carbonate depletion indicates a migration of the carbonate and so a dissolution and potentially recrystallization. The carbonates are really sensitive to water presence as well as pH change (Becze-Deak et al., 1997). It can indicate potentially a change in water concentration or in pH. The presence of water was already confirmed by the presence of intercalation and rotational pedofeatures (Fedoroff, 1997). Though, the presence of pseudomorphic crystallite coating is in direct contradiction with the intercalation and rotational structure as it needs water to be created and pseudomorphic crystallites coating are typically an indicator of semi or arid environment (Stoops George et al., 2010).

Soil Determination

To resume, this facies present plates and a lot pedofeatures related to frost action, which could indicate a gleisoil (Retallack, 2001). But the presence of a granular microstructure (Colluvial, biological and rubification origin) associate with the general reddish-brown colours are compatible with Vertisol (Retallack, 2001), even if contrary to the facies 1, this vertisoil could come from deeper Horizon. It will explain the observation of diamicton lamination, and why the channel void and in general the diversity of the porosities and biological/ surface pedofeatures (e.g. granule of biological origin) is less important compared to the N12 I to XXXVII microfacies.

For all those reasons, it is mostly possible that this facies was a Vertisoil which went by several or important frost action which transforms the soil into a gelisoil with the conservation of some characteristic of vertisoil.

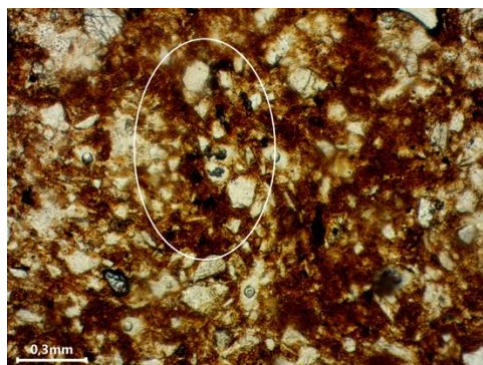


Figure 14 Link capping pedofeatures

4.2.3 Sandy mud in fine lamina-set (Facies 3)

Description:

Sandy mud in fine lamina sets are observed inside the sample 5 N16/N17 and inside the Sample 3 (inferior part), 4, 5 (Superior) and 7 22 (medium and inferior) of the columns K22, we can observe gravelly mud lamina set (Microfacies N16/N17 XIV to XX included and K22 XVIII to XXVIII included and XXXI to XXXV include) . (Annexe 1, Figure 1).

In general this facies can be separated in two parts. A matrix support part composes of complex microstructures (Vesicular/Channel) and crumbs (Figure 15), which can also be defined as some microlamination set of very well sorted sub-rounded to sub-angular silty clay to sandy silt. A variable support (matrix to clast support) presenting some crumbs and granular (Figure 15) microstructures, and which can also be defined as a horizontal lamina set of gravelly mud (Annexe 1, Figure 1).. These two parts present a different coarse material composition.

The Coarse and Fine Material

The matrix support coarse/fine relative distribution is composed of no carbonate, silicate and ferromagnesium inside the coarse to medium sand fractions and very few carbonate (5%), few silicates (10%) and very few ferromagnesium (2%) inside the fine and coarse silt fraction. The coarse material (Sand) also present a random orientation to micro-lamina formed a band with random orientation.

It also presents a diversity of fine material colours more important than the other facies, sub-facies and microfacies. Indeed, we can observe 5 different colours, brown to dark brown ; yellow-brown ; red; grey and greenish to greyish green with respectively limpid, speckles, dotted and cloudy limpidity, and a first order attenuated greyish colour interference to a high attenuates interference colours. The b-fabric is reticulate striates and parallel striated.

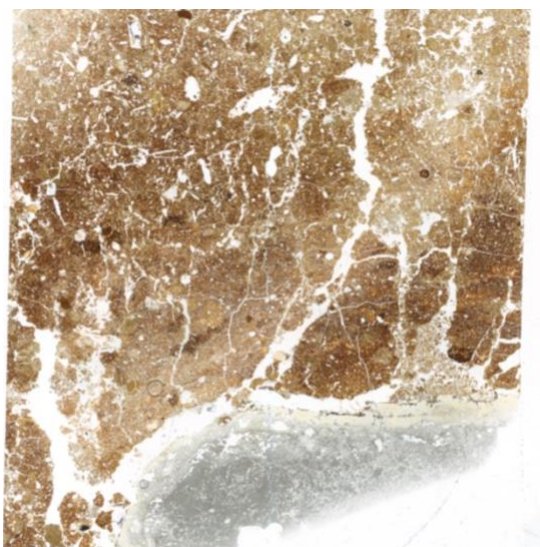
In the other hand, the variable support coarse/fine relative distribution presented very few carbonate (2-5%), very few silicates (2%) and no ferromagnesium inside the coarse to medium sand fractions and few carbonate (5-10%), few to common (20-30%) and few to very few ferromagnesium (<5%). The coarse material, gravel, present a preferential orientation which varies from none to vertical (pseudo-bands). The sand varies from microlamination to random preferred orientation . The fine material present the same colours and features that the one presented inside the general characteristic description. It also presents some reticulated striates or/ and parallel striates b-fabric.

Microstructures and pedofeatures

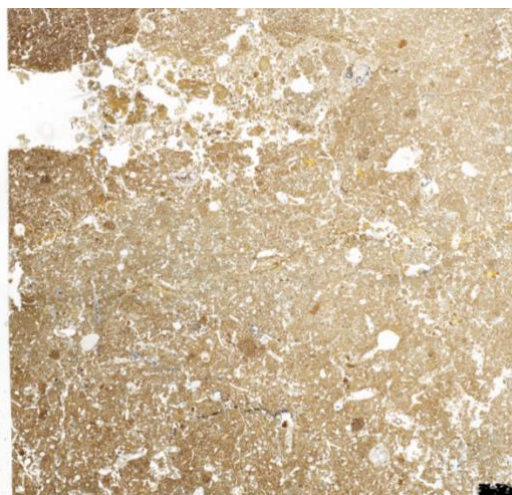
The porosities clearly identify inside this facies are vesicles; vughs; and some fissure/ crack.

Concerning the pedofeatures present inside, we can observe rotational structure; complex packing infilling, loose and discontinuous microaggregate infilling, microsparitic crystal intergrowth, are common to all the facies. The matrix support part of this facies present specific pedofeature like Fe depletion zone (Figure 16.1); microlite limpidity low refringence clay crust (Figure 16.2); speckles yellow crust (Figure 16.3); discontinuous dark red micropan (Figure 16.4) ; cryptocrystalline brownish, reddish to yellow with low refringence micropan (Figure 16.5); This macro-unit present also some sedimentary clast or rip-up clast. As limpidity clay sedimentary clasts (Figure 16.6), speckles with Fe depletion sedimentary clasts (Figure 16.7)and whitish sedimentary clasts (Figure 7.8).

The variable support part of this facies present, crystal hypocoating; dusty clay coating (Figure 10.2); crystallites coating; a discontinuous and horizontal microlayered and vesicular crust; dense and incomplete sparitic infilling discontinuous and loose complex packing. It also presents some frost action pedofeatures like discontinuous layered sorted silty clay capping.



1 (N16/N17 XX)

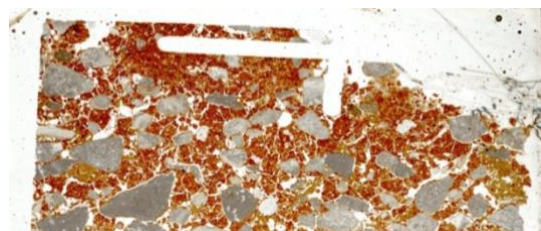


2 (N16/N17 XVII)

A



3 (K22 XXVI)



1 (K22 XX)



2 (K22 XXXV)

B

Figure 15: Halotypes of Facies 3

- A) Matrix support
- B) Variable support
 - 1) Crumns
 - 2) Complexe
 - 3) Granulars

Interpretation:

Mode of deposit and transport

This facies present some particularity and different between the two parts that compose it. First of all, the fine material colours differ from one part to the other. Secondly, we can observe that, the variable support of this facies (K22 columns) present more common features with the other facies than the Matrix support (sample 5 N16/N17).

Indeed, the matrix support part of this facies is unique compared to the other. It presents a microstratification with different fine material colours and/ or composition as well as Rip-up-clast in common quantity. They are well impregnated with a different groundmass. This indicates that they are inherited, instead of in situ formed (Karkanas & Goldberg, 2013). Indeed, the dark red micropan is rich in clay and iron with a dotted limpidity. This micropan can be associated to the other rip-up clast with the same groundmass. Those rip-up clasts can then be the result of pieces of micropan that would have been torn off.

The types of rip-up clast present inside this macro-unit are the whitish limpidity sedimentary clast could correspond to phosphate limpidity rip up clasts (Karkanas & Goldberg, 2010). They present a granular to nodular and crust, and so can be associate to Apaptite (Shahack-Gross et al., 2004; Macphail et al., 2004; Cullen, 1988). Because of all of that, we can hypothesis, that the part of this facies composing of the N16/N17 sample 5 is not a deposit facies but an erosion one.

In the other and the variable support part present a porphyric relative distribution of the coarse and fin material, the absence of gradations and it relative stratification (gravelly mud horizontal lamina set) seem to indicate water presence. It so seems to be the result of a debris flow transport even if this facies do not present diamicton.

Microstructures and pedofeatures

A new type of microstructure appears inside this facies: the Complex microstructure, vesicular/channel. The vesicular microstructure, when it is associated with various coarse and fine materials, are associated to mass material with water saturates soil material (Fedoroff et al., 2010).The channel microstructures presenting various coarse and fine materials are often associated to soil (or sediment) presenting biological activities (mostly in the sub-horizon) (Stoops George et al., 2010).

The presence of crumbs microstructures find inside this facies are also associate to surface soil like Mollisol and Vertisol (Adderley et al., 2010; Gerasimova & Lebedeva-Verba, 2010; Kovda & Mermut, 2010). It also seems coherent with the erosional description of these facies establish

above. With those informations, it is most probable that the granular microstructures present inside this facies are the result of biological activities, or rubification process instead of frost action or colluvial transport.

Concerning the pedoefeatures, a yellow speckles crust was found. It is probably a sedimentary crust, as this crust present coarse grain micro-layered formed (Stoops George et al., 2010). In that hypothesis, the vesicles result of raindrops impact (Pagliai et al., 1983a, b; Pagliai, 1987; Valentin & Ruiz Figueroa, 1987; Pagliai et al., 1989; Pagliai et al., 2004;).

It will so indicate at one point or another the presence of water, which is also indicated by the presence of iron depletion zone and the goethite, which is inside the N16/N17 sample 5 (Matrix support part of this facies very common in this part. To be more precise, it even indicates a prolonged saturated water condition (Arocena et al., 1994; PiPujol & Buurman, 1997). The variable support part (K22 columns) of this facies, the vesicular discontinuous and layered crust is classified into the sedimentary crust (Stoops George et al., 2010). Normally, vesicular crust is associate to arid or semi-arid climate (Stoops George et al., 2010) even if some layered vesicular crust, have also been observed into high montane areas or Arctic regains (Volk & Geyger, 1970).

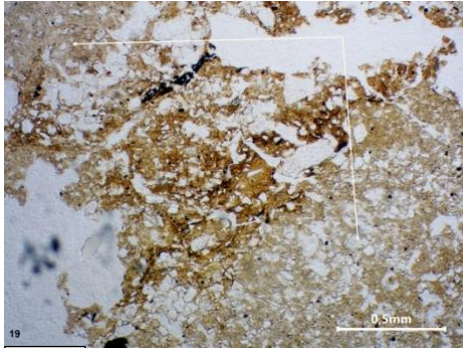
Soil Determination

As the two parts probably result from the difference process (eriosn VS depot) the types of soil composing those parts are also different. The N16/N17 sample 5, consisting of the Matrix support part of this facies is complex. It is a nested horizon. It presents some reworked clay, iron (precipitation and/or depletion form). Because of that it presents like a red soil, which class it into the Alfisol category. Thought It also present some hydromorphy reworked trace (goethite, iron depletion...), which is typical of vertisol. The concentration of the iron oxide indicates a good drainage condition like for oxisol.

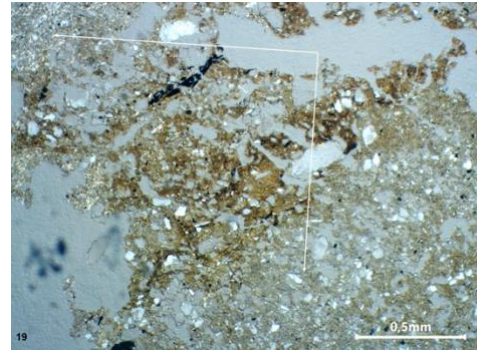
Because of all those elements, we have the hypothesis that this part of the facies (N16/N17 sample 5) is an oxisoil created from an alfisol which present more or less a reworked by mud flow.

Inversely, the variable support part of this facies (K22 columns) is way more simple. It presents a granular microstructure associate to reddish-brown colours like vertisol. As it also presents some lamina set, it is possible that this vertisol coming from deeper horizon than the one meets into the previous facies. The presence of the vesicular discontinuous crust could be the result of a little aridification compared to the other facies, sub-facies and microfacies. As this layered present also some trace of frost action, it is possible that the aridification of this macro-unit was coming more

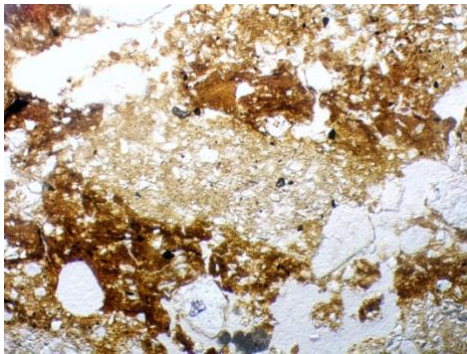
from cold environment that warm environment. So this part is probably a vertisol coming from deeper horizon which would have undergone the action of the cold leading to a slight aridification.



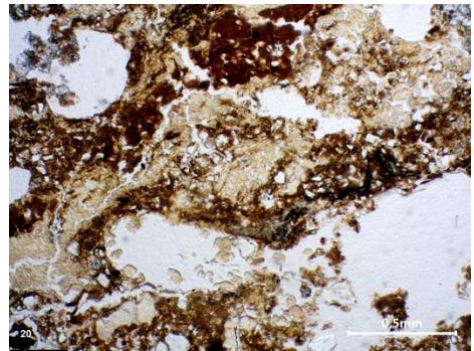
1



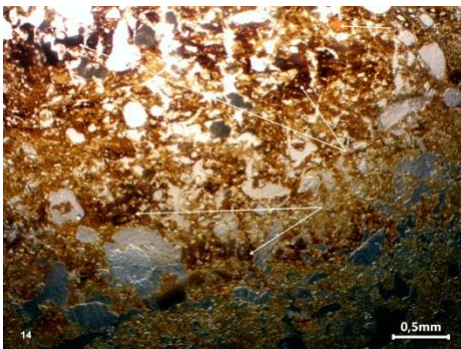
1



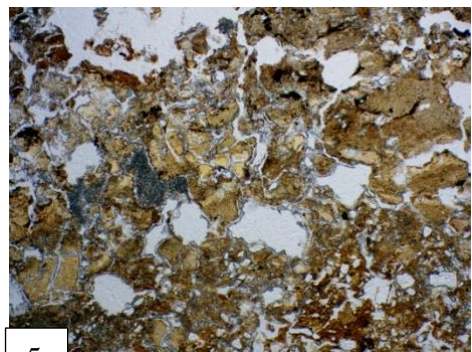
2



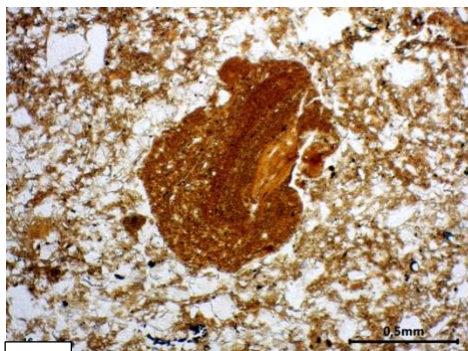
3



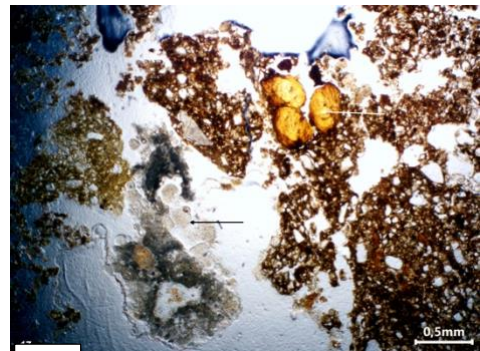
4



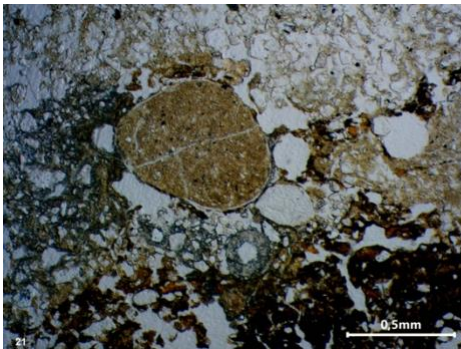
5



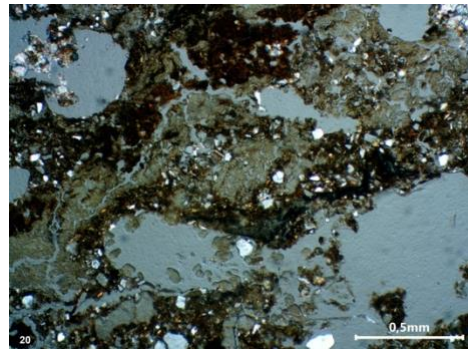
6



6



7



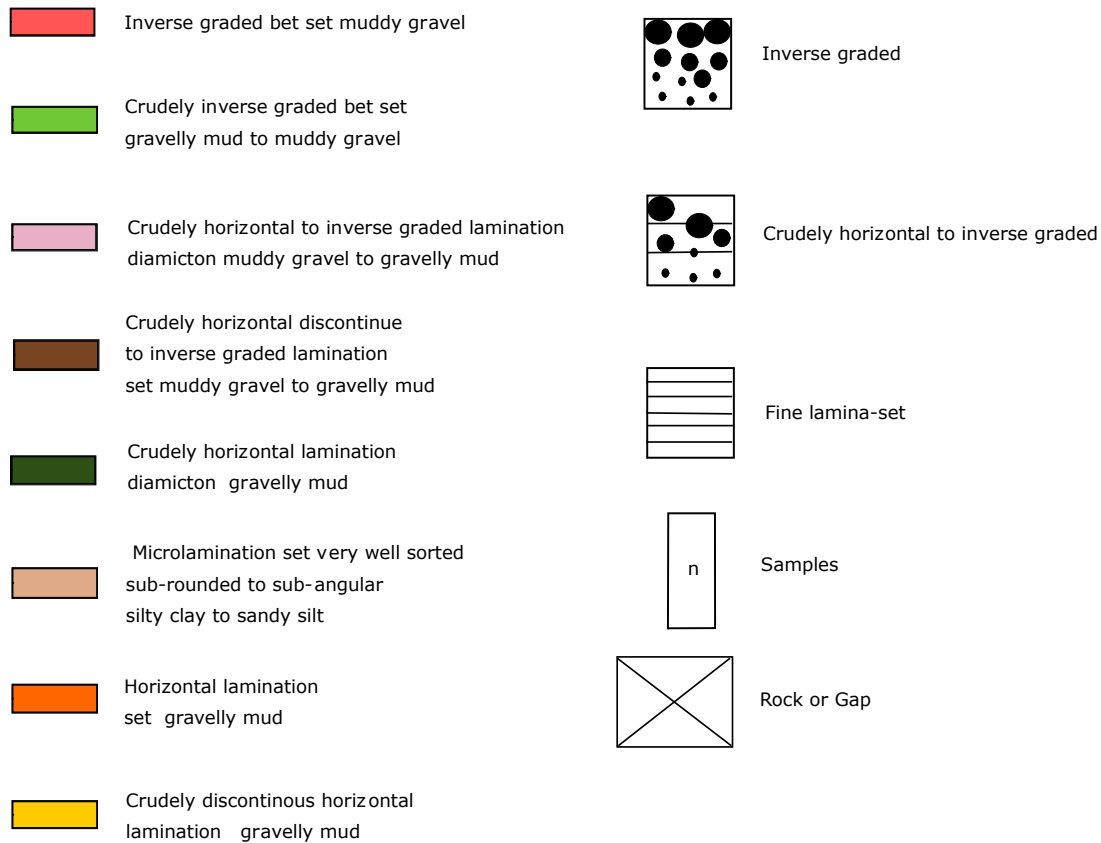
8

Figure 16: Photography of pedofeatures 3

- 1) Fe depletion zone; 2) microlite limpidity mow refringence clay crust ; 3) speckles yellow crust; 4) discontinuous dark red micropan ; 5) cryptocrystalline brownish, reddish to yellow with low refringence micropan; 6) limpidity clay sedimentary clasts; 7) speckles with Fe depletion sedimentary clasts; 8) whitish sedimentary clasts

4.3 TD 10 Resume- Stratigraphy

Figure 17: Stratigraphy Legend of the Columns N12 (A), N16/N17 (B) and K22 (C) of Gran Dolina TD-10



A synthetic tree regrouping all the microfacies present inside the Figure 18 according to the different facies, types of support are present inside the Annexe 1 (Figure 1)

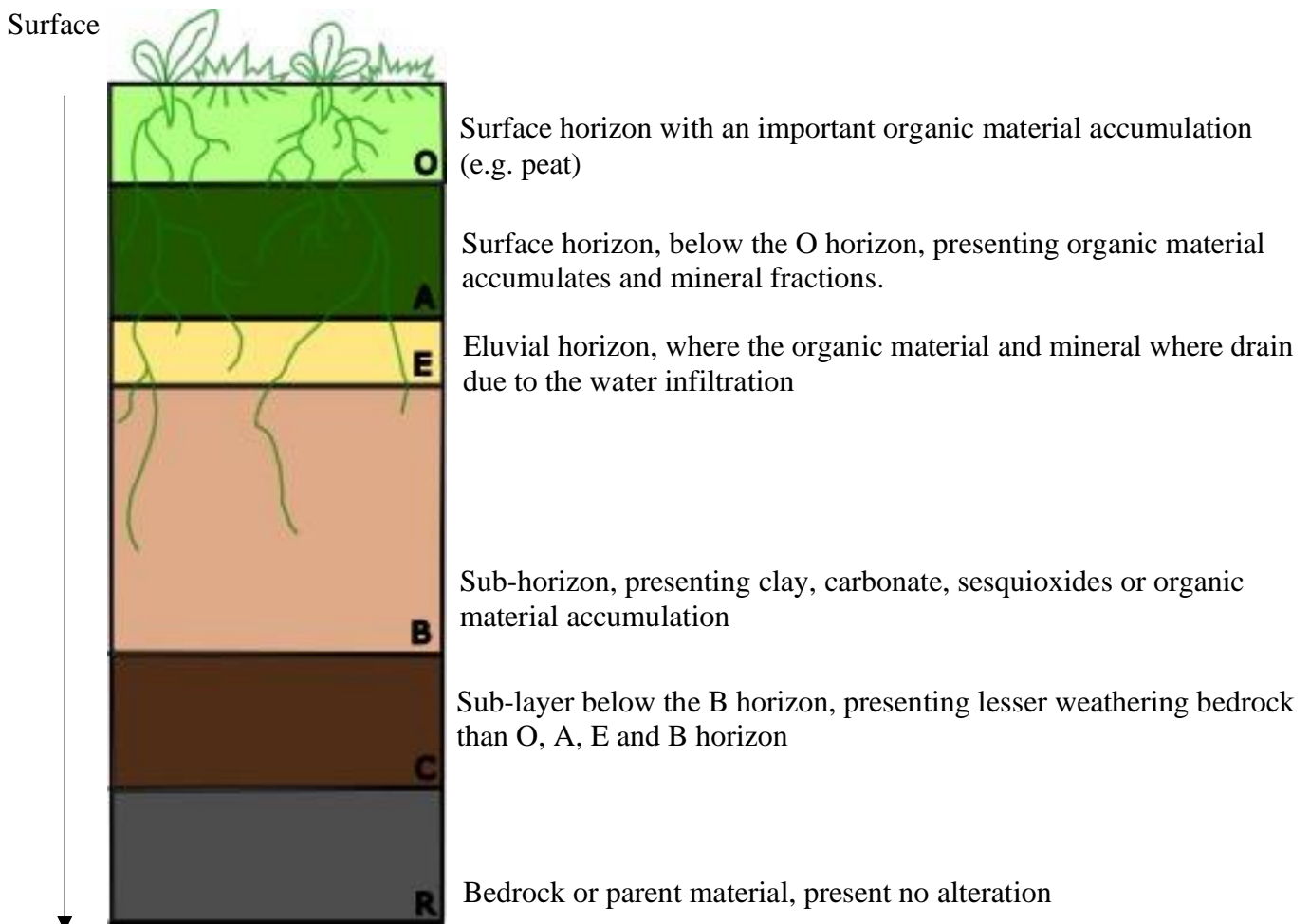
Chapter 5: Discussion

Stratigraphy to paleo-stratigraphy

TD-10 unit Soil horizon

The different microstructures and pedofeatures allow distinguishing different microfacies but also the different Horizon of paleo-soil composing the different columns. Here we used the term of paleosoil as it was defined by Stoop and al,(2010). It means that a paleo-soil, is any burial soil with a function totally or partially stop by the burial (Stoops George et al., 2010). Soil horizon can be defined as a layer presenting a specific kind and thickness (Lin, 2012). Indeed, the soil can be devised in 3 categories, the master horizon, the gradation and the subordinate (Retallack Gregory J., 2001). A modern soil is normally composed of 6 master horizon, O, A, E, B, C and R (Figure 19)

Figure 19: Schema of Soil Horizon Organisation



The surface horizon (O, A and E) presented different pedofeatures than the subsurface horizon (B, C and R), but also different pedofeatures between the surface horizons themselves. However, Finding O horizon inside a paleosol can be rarer. O horizon is constituted of leaves, needles, twigs, moss or lichen litter at different stages of decomposition (undecomposed, partially or highly) or of organic material saturated with water for a long time (Lin, 2012). Because of that, it is easy to imagine that old paleosols do not preserve O horizon, except in specific condition of preservation . Inside the TD-10 layer, for example, no O horizon was found.

The gradations horizon is horizon creating a transition between two master horizons. It presents characteristics of two master horizons, yet, one master horizon is dominant compared to the other. On the other hand, the subordinate represents a subcategory of a Horizon, as it is used to complete the description of a Horizon (Retallack Gregory J., 2001).

The different soil propriety depends mainly on the position inside the depth profile that they occupied (Jenny, 1941). The surface horizons are mainly characterized by the presence of granular microstructures, as well as pedofeatures linked to biological activity (pellets, deformation vermiform, chamber...) and the weathering process (crystallization and dissolution of carbonate, advantage degradation of minerals...). The subsurface presenting fewer pedofeatures links to biological activity and weathering, no granular or minority of granular microstructure, for example. It can also be characterized by plates, lenticular or sub-angular microstructures inside soil effect by frost (Kovda & Mermut, 2010; Stoops George et al., 2010; Van Vliet-Lanoe, 2010). Argic horizon are also typical of the subsurface horizon (Stoops George et al., 2010).

Inside the TD-10 columns, N12, N16/N17 and K22, three types of horizons have been observed, two gradations, AB and BC and one master horizon B. In addition, 7 subordinates were used to characterize the different horizon. All the different horizons, master, gradation and subordinates evoke or find inside TD-10 are listed and defined inside the table 3

Inside the columns N12 we have found, 7 horizons, 4 inside the columns N16/N17 and 16 inside the K22.

It is interesting to note that, the AB gradation, find in all tree columns, present much more diversity than the B master horizon or the BC gradation. We note 5/7 AB gradation type for the N12 columns, 4/6 for N16/N17 and 9/21 for K22.

Horizon	Definition (Retallack Gregory J., 2001)
A (no present inside TD-10)	The presence of an accumulation of organic material (humified) and mineral fraction.
B	Sub-horizon (below O, A or E) with an accumulation of clay, carbonate, sesquioxide or organic material
C (no present inside TD-10)	Sub horizon present few weathered, less than the A, E, or E horizon but more than the bedrock(R)
Gradation	Definition (Retallack Gregory J., 2001)
AB	Horizon with features of layer A and B, where A feature are dominant
BC	Horizon of transition between the B horizon and C (bedrock presenting few weathered).
Subordinate	Definition (Retallack Gregory J., 2001)
kk	Accumulation of carbonate but less than for the horizon K and more than the subordinate k
k	Accumulation of carbonate, less than the subordinate kk
f	Soil presenting frost evidence
s	Accumulation of sesquioxide resulting from illuviation process
r	Bedrock characterized by weathering or softness
t	Clay's accumulation
e	Presence of organic material in decomposition (intermediate level)
c	Presence of concretions or nodules.

Table 3: Listing and definition of the different master horizons, gradations and subordinates find or need to define the horizon present inside TD-10 units

On the other hand, the BC gradation is the less present horizon and the lesser diversity one. It is presented only inside the K22 columns (3/16). In total, we have 14 types of AB gradation, 8 types of B master horizons and 4 types of BC gradations (Annexe 1 figure 2 or figure 20) . The distribution of all those different horizons according to the microfacies define in chapter 4 are resuming inside the Annexe 1, figure 2.. We can explain the important diversity of gradation AB compared to BC gradations and B master horizon, by the types of transport and the deposit. Indeed, we have seen that the different facies are the result of colluvial deposit, grain flow, debris flow, rock fall and solifluction(Blikra & Nemec, 1998). It so corresponds to a mass movement more or less important. Those mass movement can so stop or slow the development/ function of the soil by burial them (Stoops George et al., 2010). Because of that, the soils do not have time to evolve in deeper horizon. We can also hypothese that surface soils are more sensitive to environmental change due to its position which presents more interactions with the atmosphere and biosphere. This could explain why the AB gradation present more variation than the B master horizon which presents more variation than the BC gradation, which is normally deeper than the B master horizon.

Furthermore, the horizon variation can allow to determine the evolution of the soil. Inside the pedo-stratigraphy (figure 20) we can see that several composites vary frost evidence, sesquioxide accumulation, clay accumulation, weathering, organic material. The carbonate presence is a constant even if the quantity can vary from one horizon to another. From all those composite variations, it seems that the soil formation factor which vary is climate. The clearest evidence of that is the variation of frost evidence. However, the presence of sesquioxide can also indicate a variation in climate since there is the result of alteration. The organic material variation can also be the result of climatic change, e.g. a change of horizon with an important organic material accumulation to no organic material indicate an important change like climatic. Most of the time the sesquioxide accumulations are found in the horizon which does not present frost evidence. With all that information, we can make the hypothesis that the TD-10 soil has been formed into two types of climates. Cold periods which form soil showing frost evidence e.g. cryosol or gelisol, and warm periods, the melt of the ice, help to the alteration of the soil and resulting in a sesquioxide accumulation. Because of that, we can deduce that the soil of the TD-layered has been formed in two phases, and so can be called a biphasic soil. (Stoops George et al., 2010) Indeed a biphasic soil is forms when there are a superimposition of 2 biostasy period, which is a phase with a climate favourable to soil development, are superimposed

(Stoops George et al., 2010). This could explain the different types of soils find, vertisol and Mollisol (Facies 1), Alfisol/ Oxisol (Facies 3) and gelisol (Facies 2) (see chapter 4).

TD-10-unit Soil Sequences and Classification

Thank to the determination of the different horizons, we have been able to detect the different sequences composing the 3 columns studied. According to Schaetz and Anderson (2005) a soil sequence consisted of related soil which presents gradual change due to a gradient from a dominant soil formation factor (Climat, biology, topography...). The determination of the difference sequence and their relationship allow then to classify the soil profile, which gives information about the sedimentary accumulation of the profile and the condition of its deposit (Tabor & Myers, 2015).

As we can observe in the figure 20, the different horizons present some common features, along with them kk is the most common. The subordinate f, s and t are also frequent, but their presence vary more (Figure 20). Their presence or their absence inside the horizons allows to determine the different sequences, but also to classify them.

Then, the columns N12 present four sequences. The first sequence is composed of surface horizon and one subsurface horizon which present two types of subordinate, kk that is present in all the horizon and f that vary and are only present in two horizons (Figure 20). The overprint of the characteristic of B horizon and kk subordinate could suggest that this sequence present a cumulic soil profile (Wright & Marriott, 1993). However, those soil profile should present a thick B horizon, which is not the case inside this sequence (Figure 20). This sequence present also clear defined horizon with frost features (f) and some without. This sequence can so be defined into simple soil profiles (Wright & Marriott, 1993) according to the frost characteristic. The second sequence is composed of the same horizon stop by the presence of the discordance (blue line), which create a truncator inside this sequence. As this sequence is thick and present an overprint of B horizon features, kk, f and s subordinate we can class this sequence in a cumulic soil profile (Wright & Marriott, 1993).

The third sequence of this columns is composed of only one horizon. This horizon cannot be attached to any other sequence. The truncator isolate this horizon from the sequence above and the horizons following do not correspond to the normal deposit order. It is likely that this sequence was composed of other horizons that have been eroded, hence the presence of the truncation. Without any other information, we can classify this soil profile as cumulic due to the overprinting of B horizon

characteristic (Wright & Marriott, 1993). The last sequence of this columns is composed of similar horizon, AB, presenting the same features at different degree of intensity, k/kk, (table 4) and different thicknesses, with one horizon thicker than the other (Figure 20). Therefore, we can classify this sequence as composite soil profile due to the overprinting of AB horizon in all the sequence (Wright & Marriott, 1993). The N12 columns is so composed of three types of soil profiles: cumulic/ simple, cumulic and composites. It indicates that N12 columns was formed under different sedimentary accumulation conditions. In fact, simple soil profile is formed with no sedimentary accumulation, while the cumulic soil profile is created with slow, constant and small sedimentary accumulation. On the other hand, the composite soil profile is the result of medium rapid and intermittent sedimentary accumulation. We can note that inside this columns, the intensity of sedimentary accumulation increase with the depth of the columns. It means that the intensity of sediment accumulation decreases with the time in the TD-10-unit deposit.

Concerning the N16/N17, we can also observe 4 sequences. The first sequence is defined by the presence of a discordance like the III sequence of the N12 columns. This sequence is only composed of a AB horizon. Thus, the A-B characteristic overprint all the sequence and so can be classified as a composite soil profile (Wright & Marriott, 1993). The second sequence of N16/N17 columns presents a very thick B horizon, almost half of the columns (figure 20). In addition, the different horizon of this column presents few variations. We can note frost characteristic in the bottom horizon (f), contrary to the horizon above which present clay accumulation (t) in the surface horizon composing this sequence. We can so conclude that the soil profile of this sequence is cumulic (Wright & Marriott, 1993). The two-last sequence of this column consists of a single horizon each. Even so, these two sequences are composing of AB horizon, they cannot be grouping into a single sequence to the presence of nodules or concretion inside the IV sequence (c). Those features are not in situ formed and so derive from a previous and disappeared soil. The sequences III and IV of this column are so classified into composite soil profile (Wright & Marriott, 1993). The N16/N17 is so mainly formed under slow, constants and small sedimentary accumulation as the cumulic soil occupied almost half of the N16/N17 and secondary into medium, intermittent and rapid sedimentary accumulation.

Regarding, the K22, present an important number of sequences (11) compared to the two other columns (Figure 20). The sequence I is composed of a B horizon. As it is the first horizon of the TD-10 unit and is not associate to a surface horizon, we can assume that this sequence presents a truncation above, and the surface(s) horizon(s) associated was/were eroded. The Sequences II to V present the similar characteristic between the horizon . There are composed of relatively thick AB gradations compared to the B horizons associate (Figure 20). Therefore all those sequence can be

classified as composite soil profile due to the overprinting of A-B features. (Wright & Marriott, 1993). The following sequence, VI to VII also present similar characteristics between the horizon like the sequence II to V. However, contrary to the sequence II to V, the sequences VI to VII present thicker B horizons than AB horizons associates (Figure 20). We can so conclude that those sequences are cumulic soil profiles (Wright & Marriott, 1993). The last sequence composing K22 columns, VII to XI present a new type of gradation horizon, BC, not find in the other sequences of the other columns. This gradation is closer to the parent material and presenting fewer weathering pedofeatures than the other horizon observe inside the TD-10 layer. (See table 4). Because of the presence of those horizons, which can be associate to layer of no modified material compared to the other horizons, those sequences can be associate to compound soil profiles. Those types of soil profiles are under rapid, intermittent and large sedimentary accumulation (Wright & Marriott, 1993). As this column is composed of composite and compound soil profiles, we can hypothesis that the intensity of sedimentary accumulation was more important that the columns N12 and N16/N17. K22 columns present less common characteristic than the columns N12 and N16/N17. It is probably due to the fact that the columns N12, N16/N17 and K22 are alimeted by different entries of Gran dolina cave . In fact, Gran Dolina was presenting 3 entries (Campaña et al., 2017), and so it is possible that the difference notice between the three columns, even if they belong to the same unit, are due to their different origin of entry.

To finish, the comparison between the stratigraphy and the pedo-stratigraphy (Figure 18 and Figure 20) allow the association of the different sequences with the facies define inside the chapter 4. We can observe that the distinct facies of columns N12 and N16/N17 aligns effectively with the different sequences that were observed. The Association of the facies and the sequence of the N12, and N16/N17 resume inside the table 5:

Facies	Columns N12 Sequences	Soil profile	Columns N16/N17 Sequences	Soil Profile
1	I, II	Cumulic	I	Composite
2	III, IV	Composite	II, III	Cumulic
3			IV	Composite

Table 4 : Correlation between the Facies defined inside the Chapter 3 and the different soil Sequences

We can hypothesis, that each sequence can represent an event of grain flow, which is the types of transport identify inside the columns N12 and K22 (See chapter 4). I will mean that the columns N12 was created by a minimum of four events of Grain Flow and the columns N16/N17 by a minimum of three events of Grainflow.

This association, Facies/ Sequences are not really accurate for the columns K22. Inside this column, the limit of the different Facies do not match the limit of the different sequences. It is probably due to the presence of BC gradations, which is closer to sediment than soil.

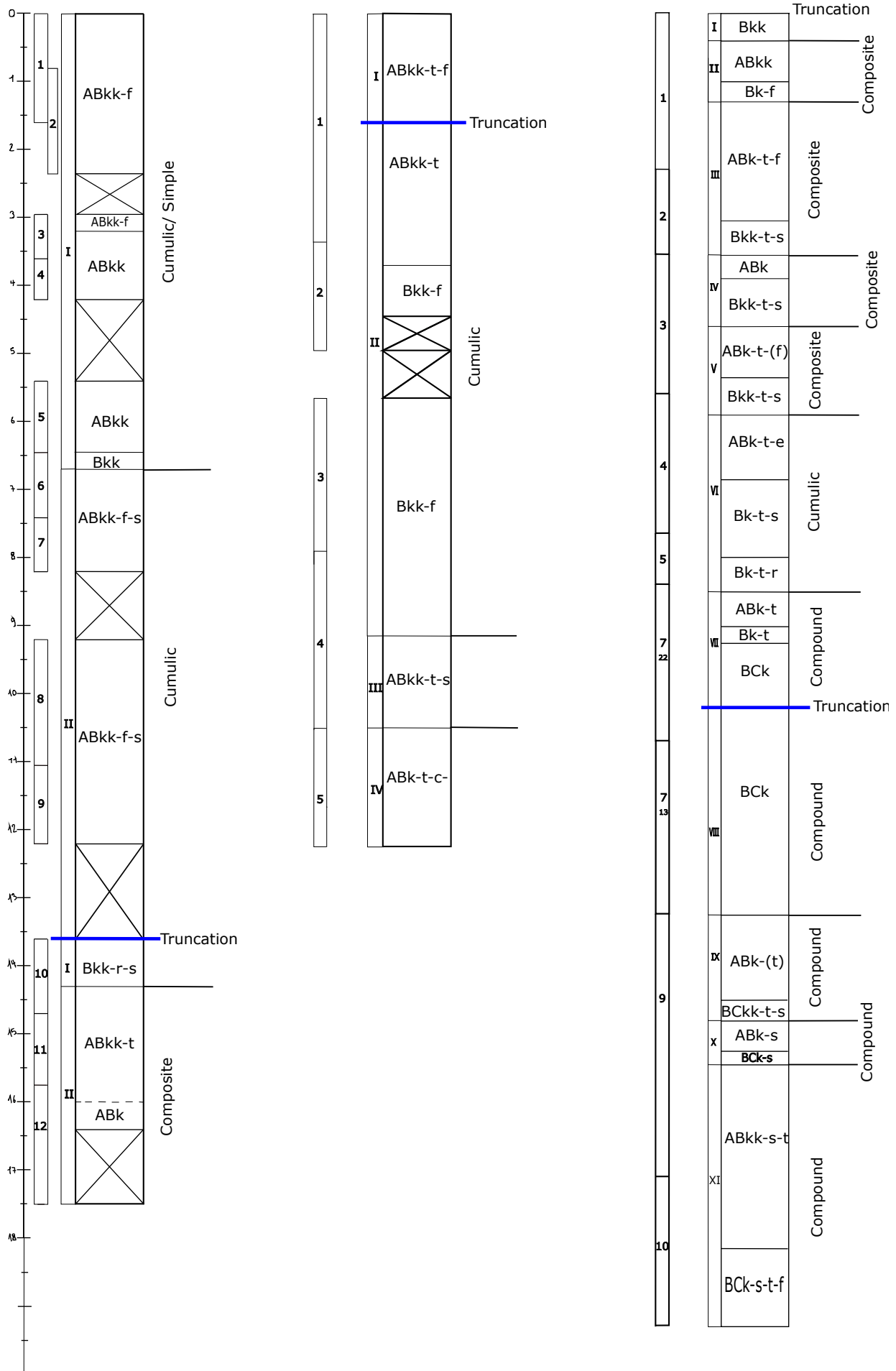


Figure 20: Pedostratigraphy of Gran Dolina TD-10 of the columns N12 (left), N16/N17 and K22 (right) Figure 20: Pedostratigraphy of Gran Dolina TD-10 of the columns N12 (left), N16/N17, and K22 (right)

TD-Unit Palaeoenvironment data

Soil data and MIS correlation

All the TD-10 soils are formed in different climate conditions. Vertisol are due to the process of wetting and drying of the clay that composes those types of soil. (Stoops George et al., 2010). The environments where there were formed is grassland to open forest (Retallack Gregory J., 2001). Mollisols can form under various temperature conditions, and so present a lot of suborder, but is usually the result of grassland environments and sometimes in open forest (Retallack Gregory J., 2001; Wilding et al., 1983). Both of them are created under sub-humid or semi-arid climate (Retallack Gregory J., 2001). The Alfisol present a lot of characteristic with the Mollisol. Indeed, there are formed under various temperatures like the Mollisol. The environment which creates vary from open forest to grassland (Retallack Gregory J., 2001).

The Oxisol are very weathering soil, and so are mostly found in climates with intense weathering like humid tropical climate, but also arid and cool environment (Ollier et Pain, 1996). Another type of soil has been found inside TD-10, the gelisol. It soil form under cold climate (Retallack Gregory J., 2001).

We have so two categories of soil found inside TD-10 units, grassland and forest soil, plus a gelisol . They result of different climates. We can assume that the grassland soil, vertisol or mollisol, could have been formed during the cold period, which could correspond to the horizon presenting frost pedofeatures (capping, granular), and for the must colder period the gelisol (plates) but also during less cold period, corresponding then to the horizon with no or weak pedofeatures.

The forest soil, alfisol and oxisol, have been identified inside the same horizon and as an oxisol derived from an alfisol (Chap 4.2.3). This means that a part of the soil forming the facies 3 representing by the sample 5 of the columns N16/N17 was formed under a warm period as no frost pedofeatures were found inside those horizons, this period was followed by a warmer and more humid period, which has transformed the Alfisol into an Oxisol. It could so explain the important presence of goethite of these samples. In fact, the goethite is forme under prolonged saturated water condition (Arocena et al., 1994; PiPujol & Buurman, 1997).

The important presence of carbonate inside all the facies (Chapter 4) and there granular formed indicated an important Taphonomical transformation. As evoke inside the Chapter 4, the carbonates are sensible to weathering. The variation of cold and warm period could have influenced the weathering process of the soil and so the presence and the shape of the carbonate present into the TD-10 layer.

When we compare the types of soil found inside our study with the stratigraphy of TD-10 layers, we can see that the Oxisol derived from the Alfisol are only present inside the TD-10.4. To be more precise it corresponds to the bottom part of the TD-10.4. The gelsol is also only found inside the TD-10.2 and TD-10.3. In the other hand, the vertisol/mollisol are found inside all the sub-layer of TD-10 (TD-10.1, TD-10.2, TD-10.3 and TD-10.4). Those data seem in contradiction with the MIS correlation. Indeed, we have established that the different sub-unit of TD-10 was associated to 2 cold periods, TD-10.1 and TD-10.4 and one warm period TD-10.3 and TD-10.2 (see chapter 1). But the presence of gelsol, formed inside cold climate, inside the TD-10.2 and TD-10.3 seem incompatible with the warm period of the MIS 11(a and b). Similarly, the presence of an oxisol, inside the TD-10.4 seem incompatible with the cold period defined by the MIS 9b. In addition, all the subunit of TD-10 seems to present the horizon with frost pedofeatures, characteristic of cold or cool climate, and horizon without, characteristic of more warm and humid climate. There are so no distribution of frost features following the repartition of the different sub-unit of TD-10. This difference, between those data can be explained by the scale. The MIS give palaeoenvironment's information for a large scale (e.g. region and more) while the study of paleosol can only give local information as the soil is the result of a local condition (e.g. hydrological system), and so influence all the palaeoenvironment interpretation by mimicking climatic condition (Driese and Ashley, 2016).

To finish, we can notice that the TD-11 presents a more yellowish colour due to the importance of carbonate in the contrary of the TD-10 layer which presents more reddish colours. We can hypothesize that, originally, the TD-10 layer could have presented a colour similar to the TD-11 layer. The processes of weathering and transformation of the soil through a rubification process could have left the TD-10 layer with less carbonate and into granular form. It is possible that the warmer and more humid period correspond to a phase of carbonate dissolution and migration. On the other hand, the colder periods could correspond to phases of recrystallization of carbonates in granular form.

TD-10 unit micro-vertebrate reconstruction

In addition to the soil palaeoenvironmental data that we have obtained, several micro-vertebrates found inside TD-10 units also give some environmental information .

According to the analysis made by Cuenca Bescós and al (2011) the TD-10-layer present 5 types of animal environments: Open and dry environments (OD), Open and humid environments (OH), Woodland, rock environments and Water-edge.

The small mammal of the OD environment represents the majority of the small mammal found inside TD-10, following by OH environments small mammals. The woodland, rock and water-edge environments small mammal represents a minority (Figure 21) (Cuenca-Bescós et al., 2011). Even so, we can observe some variation of inside the minimal number of individuals (MNI) groups. We can observe inside the figure 21, reproduce from Cuenca Bescós and al (2011) study, that every diminution of the MNI groups of OD environments, correspond to an augmentation of MNI groups of OH, woodland, rock and water-edge environments (Figure 21). However, the augmentation of woodland, rock and water-edge environments MNI groups are very little compared to the OH environments MNI groups, as from the start this type of habitat is more represented. We can observe three diminutions of the MNI groups from OD environments inside the TD-10 layer. That corresponds to three passages from an Open and dry environment to Open and Humid environments (Figure 21). It is interesting to note that inside our pedostratigraphy (Figure 20) we can observe 3 passage from cryosols to entisols and alfisols no frost affected inside the columns N12, 3 for the columns N16/N17 and 3 for K22. We can so hypothesis that during the TD-10 formation, the environments have passed from sol type(s) 1 to sol type(s) 2 in minimum tree time, as the soil and micro-vertebrate data suggest. We can so make the hypothesis that what Cuenca Bescós and al (2011) identify to OD environments correspond to what we have suggested to be a cold period, and the OH environments to the warmer period. The formation of the ice could have contributed to making the soil environments more dry, and it melting more humid. It would so create a succession of Dry and Humid environments, as the micro-vertebrate data indicate.

TD-10 unit Palynology reconstruction.

The data obtain thanks to the pollen are less accurate than the one finds thank to micro-vertebrate due to the lack of pollen inside the TD-10 layer. Indeed, pollen was found only at the base of the TD-10 (TD-10.4) and are completely absent in the other sub-layer (TD-10.3,2 and 1) of TD-10. Despite the pollen found present an important proportion of Pinus, contrary of the Mediterranean species like Olea and temperate one, e.g. deciduous Quercus are less abundant. This could indicate a transition to a cold phase (García-Anton, 1995).

TD-10.4 seem so according to pollinic data warm phase, maybe the warmer one of TD-10. It also what suggest the data obtain thank to soil study, as it is the only sub-layer where Oxisol were found. Moreover, the bottom part of all the tree columns study, N12, N16/N17 and K22, do not or weakly present frost pedofeatures. It suggests that the start of TD-10 layer deposit, TD-10.4 was a warm period.

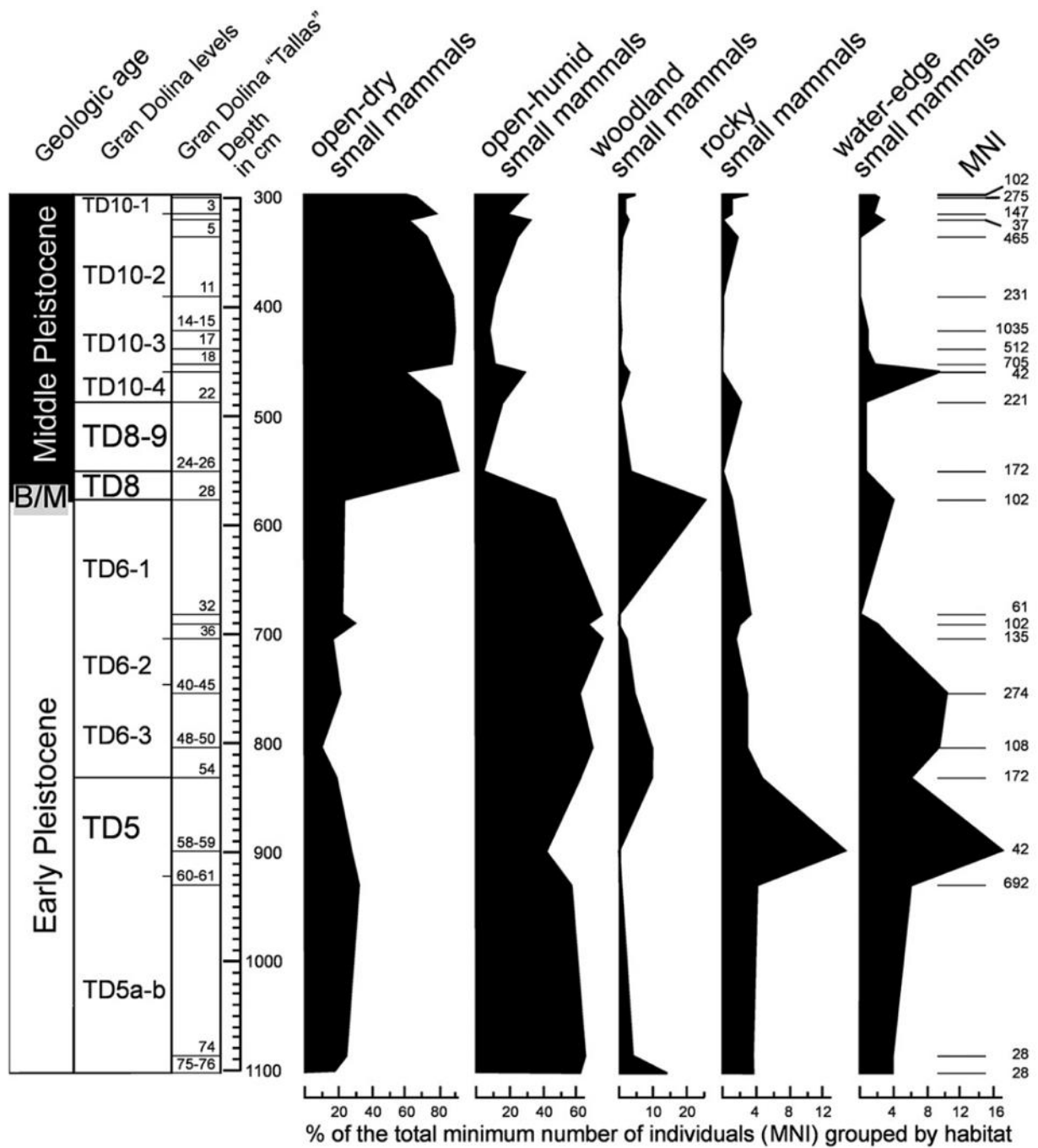


Figure 21 "Distribution of The Early Middle Pleistocene habitats of small-mammal association throughout The Gran Dolina Sequence, Sierra de Atapuerca, Burgos, Spain

(modified from Cuenca-Bescós et al., 2005) ». reproduced from "The Early-Middle Pleistocene environmental and climatic change and the human expansion in Western Europe: A case study with small vertebrates (Gran Dolina, Atapuerca, Spain)" G. Cuenca-Bescós a, M. Melero-Rubio a, J. Rofes a, I. Martínez b, J.L. Arsuaga c, H.-A. Blain d, J.M. López-García d, E. Carbonell d, J.M. Bermudez de Castro, 2011, Journal of Human Evolution p 484

Chapter 6 : Conclusion

Even if more study is needed to obtain better information about the environments, especially at the transition of cold period and warmer period with potentially other environmental data (e.g. micromorphology, stratigraphic, petrologic, micro-vertebrate...) This micromorphology analysis have allowed to determine the transport and the deposit and the climatic variation that was affecting the soil of TD-10.

In fact, thanks to the analysis of several samples coming from the two profiles of Gran Dolina site, North-east and South-East, grouping into three columns, N12, N16/N16 and K22, we have demonstrated that the TD-10 layer was created by slope deposits, more precisely by grain-flow deposits (Facies 1), debris flow (Facies 2 and 3), and very few rock falls (Facies 2). Moreover, some solifluction was also observing (Facies 2) superimpose to the initial mode of deposits.

In addition, the micromorphology was used to classify the different soil that composing the different columns through the determination of microfacies. The TD-10 layer is mainly composed of surface soil, Vertisol, Mollisol or Afisol which was going through different processes which transforms them some time into Gelisol or Oxisol. The soil profile present some cumulative, composite or compound soil sequence. It also shows a variation of the frost impact inside the soil, with microfacies showing clearly a strong characteristic of frost action (capping, plates, granular...). The soil sequences also reveal alternance of soil horizon impacted by frost action and some without. This variation was interpreted as an alternance of cold period and warmer period. Those results were in coherence with previous study realized on micro-vertebrate and pollen, which show a variation of open-dry habitat (cold period) with open-humid habitat (warm period), inside the TD-10.

To finish, the soil data obtain was compare to the environmental context give by the correlation of the Marine Isotopies Stages (MIS) and Bayesian dates model produced with previous published dates . The TD-10 units is associated to 5 different Marine isotopes Stages, 12b and a (TD-10.4), 11b (TD-10.3) , 11a (TD-10.2) and 9c (TD-10.1) .However the environment data obtain thank to the MIS correlation do not seem to match the soil data obtain. This is

probably be due to the local context associate with soil investigation, contrary to the Marine Isotopies stages.

In conclusion, we can say that the TD-10 unit still present some challenges especially with the erosional facies find inside the TD-10.4. Futures studies would be necessary to fully understand this depot and it context. The relation between TD-9 , TD-11, and TD-10, no treat inside this study, should also be considerate for furture analasys to obtain a better comprehension of TD-10 units.

Acknowledgements

The production of this master thesis and more broadly participate to the IMPQ master program have been an incredible journey.

I am deeply grateful for the European Commission for awarding me a grant and so, have make possible for me the realisation of this research and be a part of this programme.

I would like to express my sincerest gratitude to my director of master thesis, Josep Vallverdú, without whom I would never have been able to finish or even start this research. I would like to thank you for all your advice, your patience and your commitment. Learning alongside you was a real opportunity.

I would also like to thank my co-director, David M Martín Perea, who always made himself available and encouraged me during this research

I am really grateful of the Università degli Studi di Ferrara, and in particular my professors, Marta Arzarello, without whom nothing would have been possible, Julie Arnaud, Sara Daffara and Stefano Lugli, who introduced me to geo-archaeology and made me love it.

I am also very grateful to my hosting university, Universitat Rovira Virgili, and my coordinator there, Carlos Lorenzo for all their help during my mobility. I would like also acknowledge the support of the Institut of Català de Paleoecologia Humana i Evolució Social (IPHES), which have allowed me to carry out all my laboratory research. I am very grateful for the opportunity to worked there, both in the laboratory and on their archaeological sites . I met some great researchers who taught me an enormous amount.

I would also like to thank the Atapuerca Foundation for allowing me to work on one of its sites, Gran Dolina, and Ana for introducing me to the site.

Bibliography

- A**
- Adderley, W. P., Wilson, C. A., Simpson, I. A., & Davidson, D. A. (2010). Anthropogenic features. . In In Stoops, G., Marcelino, V. & Mees, F. (eds.), *Interpretation of Micromorphological Features of Soils and Regoliths*. (Elsevier, Amsterdam, pp. 569–588).
- ADEWUMI, O. L. (2019). *Soil Micromorphology of the Sedimentary Samples from Anta 1 de Vale da Laje, Tomar, Portugal* [Master Thesis]. Instituto Politécnico de Tomar.
- Arocena, J. M., Pawluk, S., & Dudas, M. J. (1994). Iron oxides in iron-rich nodules of sandy soils from Alberta (Canada). In Ringrose-Voase, A.J. & Humphreys, G.S. (eds.), *Soil Micromorphology: Studies in Management and Genesis*. In *Soil Science*,: Vol. 22. (Elsevier, Amsterdam, pp. 83-97.).
- B**
- Bates, R. L., & Jackson, J. A. (1987). *Glossary of Geology : Vol. Am. Geol. Int* (3rd edition).
- Becze-Deak, J., Langohr ~', R., & Verrecchia, E. P. (1997). Small scale secondary CaCO₃ accumulations in selected sections of the European loess belt. Morphological forms and potential for paleoenvironmental reconstruction.
- Berger, G. W., Pérez-González, A., Carbonell, E., Arsuaga, J. L., de Castro, J. M. B., & Ku, T. L. (2008). Luminescence chronology of cave sediments at the Atapuerca paleoanthropological site, Spain. *Journal of Human Evolution*, 55(2), 300-311.
- Bertran, P., & Texier, J. (1999). Facies and microfacies of slope deposits. *Catena*, 35(2–4), 99–121. [https://doi.org/10.1016/s0341-8162\(98\)00096-4](https://doi.org/10.1016/s0341-8162(98)00096-4)
- Bertran, P., Coutard, J. P., Francou, B., Ozouf, J. C., & Texier, J. P. (1992). Données nouvelles sur l'origine du lintage des grèzes: implications paléoclimatiques. . *Géographie Physique et Quaternaire*, , 46(1), 97-112.

- Bertran, P., Héту, B., Texier, J., & Van Steijn, H. (1997). Fabric characteristics of subaerial slope deposits. *Sedimentology*, 44(1), 1–16. <https://doi.org/10.1111/j.1365-3091.1997.tb00421.x>
- Birkeland, P. W. (1984). *Soils and geomorphology*. (Oxford university).
- Blain, H.-A., Bailon, S., Cuenca-Bescos, G., Arsuaga, J. L., Bermúdez de Castro, J. M., & Carbonell, E. (2009). Long-term climate record inferred from early-middle Pleistocene amphibian and squamate reptile assemblages at the Gran Dolina Cave, Atapuerca, Spain. *Journal of Human Evolution*, 56, 55–65.
- Blain, H.-A., Cuenca-Bescos, G., Lozano-Fernandez, I., Lopez-García, J. M., Olle, A., Rosell, J., & Rodríguez, J. (2012). Investigating the Mid-Brunhes Event in the Spanish terrestrial sequence. *Geology*, 40, 1051. – 1054.
- Blikra, L. H., & Nemeč, W. (1998). Postglacial colluvium in western Norway: depositional processes, facies and palaeoclimatic record. *International Association of Sedimentology*, 45, 909–959.
- Blott, S. J., & Pye, K. (2012). Particle size scales and classification of sediment types based on particle size distributions: Review and recommended procedures. *Sedimentology*, 59(7), 2071–2096. <https://doi.org/10.1111/j.1365-3091.2012.01335.x>
- Borchert, H. (1961). Einfluss der Bodenerosion auf die Bodenstruktur und Methoden zu ihrer Kennzeichnung. *Geologisches Jahrbuch*, 78, 439–502.
- Bronger, A. (1969). Zur Mikromorphogenese und zum Tonmineralbestand quartärer Loessböden Südbaden. *Geoderma* 3, 281-320.
- Bronnikova, M. A., Panin, A. V., Murasheva, V. V., & Golyeva, A. A. (2016). Soil micromorphology in archaeology: history, objectives, possibilities and prospects. *Бюллетень Почвенного института им. ВВ Докучаева*, (86), 35-45.
- Bullock, P, Fedoroff N, Jongerius A, Stoops, G, Tursina T, . (1985). *Handbook for Soil Thin Section Description*.

C

- Campaña, I., Benito-Calvo, A., Pérez-González, A., & Ortega, A. I. (2015). Pleistocene sedimentary facies of the Gran Dolina archaeo-paleanthropological site (Sierra de Atapuerca Burgos Spain). *Quaternary International*, 433, 68–84.
- Campaña, I., Benito-Calvo, A., Pérez-González, A., Ortega, A. I., Bermúdez de Castro, J. M., & Carbonell, E. (2017). Pleistocene sedimentary facies of the Gran Dolina archaeo-paleoanthropological site (Sierra de Atapuerca, Burgos, Spain). *Quaternary International*, 433, 68–84. <https://doi.org/10.1016/j.quaint.2015.04.023>
- Campy, M. 1982: *Le Quaternaire Franc-comtois: Essai Chronologique et Paléoclimatique* (Besançon, Thèse de Doctorat es Sciences naturelles, n°159, Faculté des Sciences et Techniques de l'Université de Franche-Comté)
- Candy, I., Schreve, D. C., Sherriff, J., & Tye, G. J. (2014). Marine Isotope Stage 11: Palaeoclimates, palaeoenvironments and its role as an analogue for the current interglacial. In *Earth-Science Reviews* (Vol. 128, pp. 18–51). <https://doi.org/10.1016/j.earscirev.2013.09.006>
- Carbonell, E., Bermúdez De Castro, J.M., Pares, J.M., Perez-Gonzalez, A., Cuenca- Bescos, G., Olle, A., Mosquera, M., Huguet, R., Van der Made, J., Rosas, A., Sala, R., Vallverdú, J., García, N., Granger, D.E., Martinon-Torres, M., Rodríguez, X.P., Stock, G.M., Verges, J.M., Allue, E., Burjachs, F., Caceres, I., Canals, A., Benito- Calvo, A., Díez, C., Lozano, M., Mateos, A., Navazo, M., Rodríguez, J., Rosell, J., Arsuaga, J.L., 2008. The first hominin of Europe. *Nature* 452, 465e469.
- Carbonell, E., García-Antón, M. D., Mallol, C., Mosquera, M., Ollé, A., Sahnouni, M., Sala, R., & Vergès, J. M. (1999). The TD6 level lithic industry from Gran Dolina, Atapuerca (Burgos, Spain). *Journal of Human Evolution : Production and Use*, 37, 653–693.
- Courty, M. A. (1992). Soil Micromorphology in Archaeology. *The British Academy*, 77, 39–59.
- Courty, M. A., & Fedoroff, N. (1985). Micromorphology of recent and buried soils in semi-arid region of Northwest India. *Geoderma*, 35, 287–332.

Courty, M. A., Goldberg, P., & Macphail, R. (1989). *Soils and micromorphology in archaeology*. . Cambridge: Cambridge.

Courty, M.-A. and Fedoroff, N. 1982: Micromorphology of a Holocene dwelling. *PACT* 7,

Cuenca-Bescós, G., & García, N. (2007). Biostratigraphic sucession of the early and middle pleistocene mammal faunas of the Atapuerca cave sites (Burgos, Spain). *CFS*, 259, 99–100.

Cuenca-Bescós, G., Melero-Rubio, M., Rofes, J., Martínez, I., Arsuaga, J. L., Blain, H. A., López-García, J. M., Carbonell, E., & Bermudez de Castro, J. M. (2011). The Early-Middle Pleistocene environmental and climatic change and the human expansion in Western Europe: A case study with small vertebrates (Gran Dolina, Atapuerca, Spain). *Journal of Human Evolution*, 60(4), 481–491. <https://doi.org/10.1016/j.jhevol.2010.04.002>

Cuenca-Bescos, G., Rofes, J., & Garcia-Pimienta, J. (2005). Environmental change across the Early-Middle Pleistocene transition: small mammalian evidence from the Trinchera Dolina cave, Atapuerca, Spain. . *Geological Society Special Publication* , 247, 277–286.

Cullen, D.J. (1988). Mineralogy of nitrogenous guano on the Bounty Islands, SW Pacific Ocean. *Sedimentology*, 35, 421–428.

D

Delage, A., & Lagatu, H. (1904). Sur la constitution de la terre arable. *CR Acad. Sci. Paris*, 109, 1043–1044.

Dewolf, Y., & Guillien, Y. (1962). Les paléosols des grèzes françaises. . *Comptes Rendus Sommaires de La Société Géologique de France*, 3, 90-92.

Driese, S. G., & Ashley, G. M. (2016). Paleoenvironmental reconstruction of a paleosol catena, the Zinj archeological level, Olduvai Gorge, Tanzania. *Quaternary research*, 85(1), 133-146.

E

Eggleton, R. A. (2001). *The regolith glossary*. . CRC LEME, Canberra., 144.

Emory, W. H. . (1857). Report on the United States and Mexican Boundary Survey. .

F

Falguères, C., Bahain, J. J., Yokoyama, Y., Arsuaga, J. L., de Castro, J. M. B., Carbonell, E., ... & Dolo, J. M. (1999). Earliest humans in Europe: the age of TD6 gran Dolina, Atapuerca, Spain. *Journal of human evolution*, 37(3-4), 343-352.

Fedoroff, N. (1997). Clay illuviation in Red Mediterranean soils. . *Catena*, 28, 171-189.

Fedoroff, N., & Courty, M. A. (1987). Morphology and distribution of textural features in arid and semiarid regions. In Fedoroff, N., Bresson, L.M. & Courty, M.A. (eds.), . In P. AFES (Ed.), *Micromorphologie des Sols, Soil Micromorphology*. (p. .213-219.).

Fedoroff, N., Courty, M. A., & Zhengtang Guo. (2010). Palaeosoils and relict soils. . In In Stoops, G., Marcelino, V. & Mees, F. (eds.), *Interpretation of Micromorphological Features of Soils and Regoliths*, (Elsevier, Amsterdam, pp. 623-662.).

Fisher, P.F. and Macphail, R.I. 1985: Studies of archaeological soils and deposits by micromorphological techniques. In Feiller, N., Gilbertson, D.D. and Ralph, N.G.A. (editors), *Palaeoenvironmental Investigations: Research Design, Method and Data Analysis* (Oxford, British Archaeological Reports International Series 258) 93-112

FitzPatrick, E. A. (2012). *Micromorphology of Soils*. Springer Science & Business Media.

Friesem, D. E., Tsartsidou, G., & Karkanas, P. et al. (2014). Where are the roofs? A geo-ethnoarchaeological study of mud structures and their collapse processes, focusing on the identification of roofs. . *Archaeological and Anthropological Science* , 6, 73-92.

Friesem, D., Boaretto, E., & Eliyahu-Behar, A. et al. (2011). Degradation of mud brick houses in an arid environment: A geoarchaeological model. . *Journal of Archaeological Science* , 38, 1135–1147.

G

- García-Anton, M. (1995). Paleovegetacion del Pleistoceno Medio de Atapuerca a través del análisis polínico. . In In: Bermúdez de Castro, J.M., Arsuaga, J.L., Carbonell, E. (Eds.), Evolucion Humana En Europa Y Los Yacimientos de La Sierra de Atapuerca. Junta de Castilla y Leon, Valladolid, (pp. 47–165).
- Gé, T., & Guilloire, P. (1993). Micromorphologie des sédiments de la salle des peintures de la Grande Grotte d'Arcy-sur-Cure, premiers résultats.. Bulletin de La Société Préhistorique Française, , 5–8.
- Gerasimova, M., & Lebedeva-Verba, M. (2010). Topsoils - mollic, takyric and yermic horizons. In In Stoops, G., Marcelino, V. & Mees, F. (eds.), Interpretation of Micromorphological Features of Soils and Regoliths. (Elsevier, Amsterdam, pp. 351–368).
- Gil, E., Aguirre, E., & Hoyos, M. (1987). Contexto estratigráfico. In: Aguirre, E, Carbonell, E., Bermúdez de Castro, J.M (Eds), El Hombre Fósil de Ibeas y El Pleistoceno de La Sierra de Atapuerca, Valladolid, Junta de Castilla y León, Consejería de Cultura y Bienestar Social, 45–47.
- Goldberg, P. 1979: Micromorphology of Pech de l'Aze 11 sediments. Journal of Archaeological Science 6, 1747.
- Goldberg, P. 1981: Applications of micromorphology in archaeology. In Bullock, P. and Murphy, C.P. (editors), Soil Micromorphology. Vol. I : Techniques and Applications (Berkhamstead, A.B. Academic Publishers) 139-150.
- Goldberg, Paul., & Macphail, Richard. (2006). Practical and theoretical geoarchaeology: Vol. chap 10. Blackwell Pub.
- Guillien, Y. (1951). Les grèzes litées de Charente. . Revue Géographique Des Pyrénées et Du Sud-Ouest. Sud-Ouest Européen, , 22(2), 154-162.
- Guilloire, P. (1980) Method de fabrication mecanique et an serie de lames minces. Department des soils, Institut National Agronomique, Grignon, Paris

H

Holmes, A. (1965). Principles of Physical Geology : Vol. 3rd edition (Thomas Nelson).`

Hoyos, M., & Aguirre, E. (1995). EL PALEOCLIMATE RECORD OF PLEISTOCENE IN THE EVOLUTION OF ATAPUERCA KARST (BURGOS): «GRAN DOLINA» SECTION. TRABAJOS DE PREHISTORIA, 2, 31–45. <http://tp.revistas.csic.es>

Hoyos, P. A., & Cortés, F. C. (1981). El poblado argárico de la Terrera del Reloj (Dehesas de Guadix, Granada). . Cuadernos de Prehistoria y Arqueología de La Universidad de Granada, ., 6, 257–286.

Hsü, K. J. (1975). Catastrophic debris streams (strurzstroms) generated by rockfall. Geological Society If America Bulletin , 86, 129–140.

J

Jongerius, A., & Heinzberger, G. (1975). Methods in soil micromorphology. A technique for the preparation of large thin sections. Soil Survey Institute, Wageningen, the Netherlands, 10, 1–30.

Journaux, A. (1976). Les grèzes litées du Châtillonnais. Quaternaire, , 13(3), 123-138.

K

Karkanias, P., & Efstratiou, N. (2009). Floor sequences in Neolithic Makri, Greece: micromorphology reveals cycles of renovation. Antiquity, , 83(322), 955-967.

Karkanias, P., & Goldberg, P. (2010). Phosphatic features. . In In Stoops, G., Marcelino, V. & Mees, F. (eds.), Interpretation of Micromorphological Features of Soils and Regoliths. (Elsevier, Amsterdam, pp. 521–541).

Karkanias, P., & Goldberg, P. (2013). Micromorphology of Cave Sediments. In Treatise on Geomorphology: Volume 1-14 (Vols. 1–14, pp. 286–297). Elsevier. <https://doi.org/10.1016/B978-0-12-374739-6.00120-2>

Karkanias, P., & Goldberg, P. (2018). Reconstructing archaeological sites: understanding the geoarchaeological matrix. (John Wiley & Sons.).

- Kemp, R. A. (1995). Distribution and genesis of calcitic pedofeatures within a rapidly aggrading loess- paleosol sequence in China. . *Geoderma* , 65, 303-316.
- Khatwa, A., & Tulaczyk, S. . (2001). Microstructural interpretations of Modern and Pleistocene subglacially deformed sediments: the relative role of parent material and subglacial process. . *Journal of Quaternary Science* , 16, 507–517.
- Kovda, I., & Mermut, A. (2010). Vertic features. In Stoops, G., Marcelino, V. & Mees, F. (eds.), . In *Interpretation of Micromorphological Features of Soils and Regoliths*. (Elsevier, Amsterdam, pp. 109–127).
- Kubiëna, W. L. . (1953). *The Soils of Europe*. Thomas Murby & Co., London, 318.
- Kubiëna, W. L. (1948). *Entwicklungslehre des Bodens*. . Springer-Verlag, Wien, 215.
- Kühn, P. (2003). Spätglaziale und holozäne Lessivé´ genese auf jungweichselzeitlichen Sedimenten Deutschlands., . *Greifswalder Geographische Arbeiten* , 28, 167.
- Kühn, P., Aguilar, J., & Miedema, R. (2010). Textural pedofeatures and related horizons. . In In Stoops, G., Marcelino, V., and Mees, F. (eds), *Interpretation of Micromorphological Features of Soils and Regoliths*. (Amsterdam: Elsevier., pp. 217–250).

L

- Lachniet, M. S., Larson, G. J., Lawson, D. E., Evenson, E. B., & Alley, R. B. . (2001). Microstructures of sediment flow deposits and subglacial sediments: a comparison. . *Boreas*, 30, 254-262.
- Lachniet, M. S., Larson, G. J., Strasser, J. C., Lawson, D. E., & Evenson, E. B. (1999). Microstructures of glacial sediment flow deposits, Matanuska Glacier, Alaska. In: Mickleson, D.M., Attig, J.W. (Eds.), *Glacial Processes Past and Present*. Special paper, . . Geological Society of America, Boulder, CO, 337.

Laville, H. 1976: Deposits in calcareous rockshelters: analytical methods and climatic interpretation. In Davidson, D.A. and Shackley, M.L. (editors), *Geoarchaeology* (London, Duckworth) 137-155.

Lenoble, A. (2005). Ruissellement et formation des sites préhistoriques. Référentiel actualiste et exemple d'application au fossile,. Oxford : British Archaeological Report Internationala, 1363.

Lin, H. (2012). Understanding soil architecture and its functional manifestation across scales. In *Hydropedology: Synergistic Integration of Soil Science and Hydrology* (pp. 41–74). Elsevier. <https://doi.org/10.1016/B978-0-12-386941-8.00002-2>

M

Macphail, R. I., & Gilberg, P. (1995). Recent advances in micromorphological interpretations of soils and sediments from archaeological sites. . In In Barham and A.J and Macphail R. I (eds). *Archaeological sediment and soils: Analysis, Interpretation and Managements*. (University College).

Macphail, R.I., Cruise, G.M., Allen, M.J., Linderholm, J. and Reynolds, P. (2004). Archaeological soil and pollen analysis of experimental floor deposits; with special reference to Butser Ancient Farm, Hampshire, UK. *Journal of Archaeological Science*, 31, 175–191.

McBurney, French, & Rajkovic. (s.d.). A step by step guide ro the making of soil thin section. University of Cambridge.

Melosh, H. J. (1987). The mechanics of large rock avalanches. In Costa, J.E., Wieczorek, G.F. Eds. , *Debris FlowsrAvalanches: Process, Recognition and Mitigation* , Geological Society of America, *Reviews in Engineering Geology* , 7, 41–50.

Mentzer, S. M. (2014). Microarchaeological Approaches to the Identification and Interpretation of Combustion Features in Prehistoric Archaeological Sites. In *Journal of Archaeological Method and Theory* (Vol. 21, Issue 3, pp. 616–668). Springer New York LLC. <https://doi.org/10.1007/s10816-012-9163-2>

- Menzies, J. . (1998). Microstructures within subglacial diamictons. In: Kostrzewski, A. (Ed.), *Relief and Deposits of Present-day and Pleistocene Glaciation of the Northern Hemisphere—selected problems*. . Adam Michiewicz University Press, Geography Series, Poznan, 58, 210-216.
- Menzies, J. . (2000). . Micromorphological analyses of microfabrics and microstructures indicative of deformation processes in glacial sediments. . In: Maltman, A.J., Hubbard, B., Hambrey, J.M. (Eds.), *Deformation of Glacial Materials*. Geological Society, London, Special Publications, 176, 245–257.
- Miedema, R. (2002). Alfisol. In *Encyclopedia of Soil Science* (pp. 45–49). Alfisols.
- Miller, B. A. , & Juilleret, J. (2020). The colluvium and alluvium problem: Historical review and current state of definitions. . *Earth-Science Reviews*, , 209, 103316.
- Moreno, D., Falgueres, C., Pérez-González, A., Voinchet, P., Ghaleb, B., Desprieé, J., ... & Arsuaga, J. L. (2015). New radiometric dates on the lowest stratigraphical section (TD1 to TD6) of Gran Dolina site (Atapuerca, Spain). *Quaternary Geochronology*, 30, 535-540.
- Mücher, C. A. , Klijn, J. A., Wascher, D. M., & Schaminée, J. H. (2010). A new European Landscape Classification (LANMAP): A transparent, flexible and user-oriented methodology to distinguish landscapes. . *Ecological Indicators*, , 10(1), 87-103.
- Mücher, H. J., & De Ploey, J. (1977). Experimental and micromorphological investigation of erosion and redeposition of loess by water. *Earth Surface Processes*, , 2(2-3), 117-124.
- Mücher, H. J., & Vreeken, W. J. (1981). (Re) deposition of loess in southern Limbourg, The Netherlands. 2. Micromorphology of the Lower Silt Loam complex and comparison with deposits produced under laboratory conditions. . *Earth Surface Processes and Landforms*, , 6(3-4), 355-363.
- Muecher, H. J. (1974). Micromorphology of slope deposits: the necessity of a classification. *Soil Microscopy*, 553-566.

N

Nichols, G. (2009). . Sedimentology and stratigraphy.: Vol. second edition (John Wiley & Sons).

O

Olivé, A., Ramirez Merino, J. L., & Ortega, L. I. (1990). Mapa Geológico de España a escala 1/50 000. Belorado, 201, ITGE, Madrid.

Ollier, C., & Pain, C. (1996). Regolith, soils and landforms. John Wiley & Sons.

Ortega, A. I. (2009). La Evolucion Geomorfol ogica Del Karst de La Sierra de Atapuerca (Burgos) y Su Relaci on Con Los Yacimientos Pleistocenos Que Contiene. . Universidad de Burgos Facultad de Humanidades y Educacion.

Ortega, A. I., Benito-Calvo, A., Perez-Gonzalez, A., Martín-Merino, M. A., Perez- Martínez, R., Pares, J. M., Aramburu, A., Arsuaga, J. L., Bermúdez de Castro, J. M., & Carbonell, E. . (2013). Evolution of multilevel caves in the Sierra de Atapuerca (Burgos, Spain) and its relation to human occupation. . Geomorphology, 196, 122-133.

Ortega, A. I., Calvo, A. B., Pcrez-Gonzbleza, A., Partsb, M., Carbonellc, E., Aleixandred, T., Benitoa, A., Angel, M., & Merinof, M. (2017). L'Anthropologie 105 (2001) 27-43 0 2001 hditions scientifiques et medicales Elsevier SAS. Tous droits r&ervts G6ologie de la Sierra de Atapuerca et stratigraphie des remplissages karstiques de Galeria et Dolina (Burgos, Espagne). <https://www.researchgate.net/publication/313711516>

Ortega, A.I., Benito-Calvo, A., Perez-Gonzalez, A., Carbonell, E., Bermúdez de Castro, J.M., Arsuaga, J.L., (2014). Atapuerca Karst and its palaeoanthropological sites. In: Gutierrez, F., Gutierrez, M. (Eds.), Landscapes and Landforms of Spain, World Geomorphological Landscapes. Springer ScienceeBusiness Media Dor- drecht, pp. 101e110.

P

Palumbo, E., Flores, J. A., Perugia, C., Petrillo, Z., Voelker, A. H. L., & Amore, F. O. (2013). Millennial scale coccolithophore paleoproductivity and surface water changes between 445 and 360 ka (Marine Isotope Stages 12/11) in the Northeast Atlantic. . Palaeogeography, Palaeoclimatology, Palaeoecology. , 383/384, 27–41.

- Pagliai, M., 1987. Effects of different management practices on soil structure and surface crusting. In Fedoroff, N., Bresson, L.M. & Courty, M.A. (eds.), *Micromorphologie des Sols, Soil Micromorphology*. AFES, Paris, pp. 415–422.
- Pagliai, M., Bisdom, E.B.A., & Ledin, S., 1983a. Changes in surface structure (crusting) after application of sewage sludges and pig slurry to cultivated agricultural soils in northern Italy. *Geoderma* 30, 35–53.
- Pagliai, M., La Marca, M., & Lucamante, G., 1983b. Micromorphometric and micromorphological investigations of a clay loam soil in viticulture under zero and conventional tillage. *Journal of Soil Science* 34, 391–403.
- Pagliai, M., Pezzarossa, B., Mazzoncini, M., & Bonari, E., 1989. Effects of tillage on porosity and micro-structure of a loam soil. *Soil Technology* 2, 345–358.
- Pagliai, M., Vignozzi, N. & Pellegrini, S., 2004. Soil structure and the effect of management practices. *Soil & Tillage Research* 79, 131–143.
- Parés, J. M., & Pérez-González. (1999). Magnetostratigraphy and stratigraphy at Gran Dolina section, Atapuerca (Burgos, Spain) . *Journal of Human Evolution* .
- Phillips, E. (2006). Micromorphology of a debris flow deposit: evidence of basal shearing, hydrofracturing, liquefaction and rotational deformation during emplacement. *Quaternary Science Reviews*, 25(7–8), 720–738. <https://doi.org/10.1016/j.quascirev.2005.07.004>
- Pineda, A., & Arce, J. M. (1997). Mapa geológico de España a escala 1/ 50 000 (Burgos, 200) . I.T.G.E, Madrid.
- PiPujol, M. D., & Buurman, P. (1997). . Dynamics of iron and calcium carbonate redistribution and palaeo- hydrology in middle Eocene alluvial paleosols of the southeast Ebro Basin margin (Catalonia, north- east Spain). . *Palaeogeography, Palaeoclimatology, Palaeoecology*, 134, 87-107.

R

Regattieri, E., Giaccio, B., Galli, P., Nomade, S., Peronace, E., Messina, P., Sposato, A., Boschi, C., & Gemelli, M. (2016). A multi-proxy record of MIS 11-12 deglaciation and glacial MIS 12 instability from the Sulmona basin (central Italy). *Quaternary Science Reviews*, 132, 129–145. <https://doi.org/10.1016/j.quascirev.2015.11.015>

Retallack. (2001). Soil classification . In *Soils of the Past: An introduction to Paleopedology: Vol. second edition* (Blackwell science, pp. 63–76).

Rodríguez-Tovar, F. J., Dorador, J., & Hodell, D. A. V. (2019). Trace fossils evidence of a complex history of nutrient availability and oxygen conditions during Heinrich Event 1". . *Global and Planetary Change*. , 174, 26–34.

Rodríguez, J., Burjachs, F., Cuenca-Bescos, G., García, N., Van der Made, J., Perez González, A., Blain, H.-A., Exposito, I. , , Lopez-García, J. M., GarcíaAntón, M., Allue, E., Cáceres, I., Huguet, R., Mosquera, M., Olle, A., Rosell, J., Pare s, J. M., Rodríguez, X. P., Díez, C., ... Carbonell, E. (2011). One million years of cultural evolution in a stable environment at Atapuerca (Burgos, Spain). . *Quaternary Science Reviews* , 30 (11e12), 1396-1412.

S

Schaetz, R. J., & Anderson, A. S. (2005). *Soils: Genesis and geomorphology*. Cambridge, UK: Cambridge University Press.

Schott, H. W., Nyman, C. F., & Kotschy, T. (1854). . *Analect. bot* . . Gerold., Vol. 1.

Sehgal, J. L., & Stoops, G. (1972). Pedogenic calcic accumulation in arid and semiarid regions of the Indo-Gangetic alluvial plain of the erstwhile Punjab (India). Their morphology and origin. , . *Geoderma*, 8, 59–72.

Shahack-Gross, R. (2017). Archaeological formation theory and geoarchaeology: State-of-the-art in 2016. *Journal of Archaeological Science*, 79, 36-43.

Stein, J.K. 1985: Interpreting sediments in cultural settings. In Stein, J.K. and Farrand W.R. (editors), *Archaeological Sediments in Context* (Orono, Center for the Study of Early Man) 5-19.

Stoops George, Marceline Vera, & Mees Florias. (2010). Interpretation of Micromorphological Feature of Soil and Regoliths.

Stoops, G., Marcelino, V., & Mees, F. (2010). Interpretation of Micromorphological Features of Soils and Regoliths. Elsevier.

Stoops, G., Vepraskas, M., & Jongmans, A. (2003). Guidelines for Analysis and Description of Soil and Regolith Thin Sections. ResearchGate. https://www.researchgate.net/publication/40127481_Guidelines_for_Analysis_and_Description_of_Soil_and_Regolith_Thin_Sections

T

Tabor, N. J., & Myers, T. S. (2015). Paleosols as Indicators of Paleoenvironment and Paleoclimates. *Earth Planet Science*, 43, 333–361.

V

Valentin, C. & Ruiz Figueroa, J.F., 1987. Effect of kinetic energy and water application rate on the development of crusts in a fine sandy loam soil using sprinkling irrigation and rainfall simulation. In Fedoroff, N., Bresson, L.M. & Courty, M.A. (eds.), *Micromorphologie des Sols, Soil Micromorphology*. AFES, Paris, pp. 401–408.

Van der Meer, J. J. M. (1993). Microscopic evidence of subglacial deformation. *Quaternary Science Reviews*, 12, 553-587.

Van der Meer, J. J. M. (1997). Particle aggregate mobility in till: microscopic evidence of subglacial process. *Quaternary Science Reviews*, 16, 827–831.

Van Vliet-Lanoë, B. (1987). Dynamique périglaciaire actuelle et passée: apport de l'étude micromorphologique et de l'expérimentation. *Bulletin de l'Association Française Pour l'étude Du Quaternaire*, 24(3), 113–132. <https://doi.org/10.3406/quate.1987.1839>

Van Vliet-Lanoe, B. (2010). . Frost action. . In In Stoops, G., Marcelino, V. & Mees, F. (eds.), Interpretation of Micromorphological Features of Soils and Regoliths. (Elsevier, Amsterdam, pp. 81-108.).

Voelker, A. H. L., Rodrigues, T., Billups, K., Oppo, D., McManus, J., Stein, R. ., Hefter, J., & Grimalt, J. O. (2010). Variations in mid-latitude North Atlantic surface water properties during the mid-Brunhes (MIS 9–14) and their implications for the thermohaline circulation. . *Climate of the Past* , 6, 531–552.

Volk, O. H., & Geyger, E. (1970). . “Schaumboden” als Ursache der Vegetationslosigkeit in ariden Gebieten. . *Zeitschrift Für Geomorphologie* , 14, 79-95.`

W

Washburn. (1979). *Geocryology. A survey of periglacial processes and environment* (Arnold).

Webb, S. (2013). Australia and the Quaternary Ice Ages. In *Corridors to Extinction and the Australian Megafauna* (pp. 127–148). Elsevier. <https://doi.org/10.1016/b978-0-12-407790-4.00006-9>

Wright, V. P., & Marriott, S. B. (1993). The sequence stratigraphy of fluvial depositional systems: the role of floodplain sediment storage. . *Sedimentary Geology*, 86(3-4), 203-210.

Wu, T., Cheng, A., Lin, H., Hailin Zhang, & Yi Jie. (2023). Climatic Fluctuation of Marine Isotope Stage 9: A Case Study in the Southern Margin of the Chinese Loess Plateau. . *Journal of Earth Science*.

Annexes 1

		N12	N16/N17	K22	Halotype	
Invers grading	No	Openwork to Clast Support <ul style="list-style-type: none"> Gravelly-Crumbs Gravelly-Granular Gravelly- Sub-Granular 	I,X,XI,XXI		XV,XVI	N12 I
		Facies 1 <ul style="list-style-type: none"> Openwork to Matrix Support <ul style="list-style-type: none"> Gravelly-Crumbs Gravelly-Granular Gravelly- Sub-Granular 	II, III, IV, V,XVIII,XIX,XX		II,III,IV,V,VII,VIII,IX,XII,XIII	N12 XX
		Matrix to Openwork Support <ul style="list-style-type: none"> Gravelly-Crumbs Gravelly-Granular Gravelly- Sub-Granular 	VI,VII,VIII,IX,XVII,XXII		I,VI,X,XI,XIV,XVIII	N12 VII
Crudely stratified	Yes	Matrix Support <ul style="list-style-type: none"> muddy-Granular muddy-Plates 	XI,			N12 XI
		Facies 2 <ul style="list-style-type: none"> Variable Support <ul style="list-style-type: none"> muddy-Granular muddy-Plates 	XII,XIII,XIV,			N12 XIV
		Variable Support <ul style="list-style-type: none"> Gravelly-Crumbs Gravelly-Granular Gravelly- Sub-Granular 	XV,XVI,			N12 XV
Micro-Stratified	No	Matrix Support <ul style="list-style-type: none"> Crumbs Complexe 	XXXIII,XXXIV			N12 XXXIV
		Facies 3 <ul style="list-style-type: none"> Matrix Support <ul style="list-style-type: none"> Crumbs Complexe 	XXXIV,XXXV,XXXVI,XXVII,XXVIII,XXIX, XXX,XXXI,XXXII,XXXV,XXXVI, XXXVII,XXXVIII,XXXIX	I,II,III,IV	XXXIX,XXX	N16/N17 II
		Variable Support <ul style="list-style-type: none"> Granular Crumbs Complexe 	XXXIV,XXXV,XXXVI,XXVII,XXVIII,XXIX, XXX,XXXI,XXXII,XXXV,XXXVI, XXXVII,XXXVIII,XXXIX		XXXVI	
Invers grading	Yes	Matrix Support <ul style="list-style-type: none"> muddy-Granular muddy-Plates 	XL,XLI,XLII,XLIII		XXXVII,XXXVIII,XXXIX,XL,XLI	K22 XXXIX
		Facies 2 <ul style="list-style-type: none"> Variable Support <ul style="list-style-type: none"> muddy-Granular muddy-Plates 		VII,VIII,IX,X,XI,XIII	L,LI,LII	N16/N17 VIII
		Variable Support <ul style="list-style-type: none"> muddy-Granular muddy-Plates 		V,VI,VII,	XII,XLIII,XLIV,XLV,, XLVI,XLVII,XLVIII,XLIX,	
Micro-Stratified	No	Matrix Support <ul style="list-style-type: none"> Crumbs Complexe 				N16/N17 XII
		Facies 3 <ul style="list-style-type: none"> Matrix Support <ul style="list-style-type: none"> Crumbs Complexe 		XVIII,XIX,XX		N16/N17 XX
		Variable Support <ul style="list-style-type: none"> Granular Crumbs Complexe 		XIV,XV,XVI,XVII		N16/N17 XVII
Micro-Stratified	No	Matrix Support <ul style="list-style-type: none"> Crumbs Complexe 				N16/N17 XX
		Facies 3 <ul style="list-style-type: none"> Matrix Support <ul style="list-style-type: none"> Crumbs Complexe 		XVIII,XIX,XX		N16/N17 XX
		Variable Support <ul style="list-style-type: none"> Granular Crumbs Complexe 		XVIII,XXVI,XXXI,XXXII,XXXIII,XXXIV		K22 XXVI
Micro-Stratified	No	Matrix Support <ul style="list-style-type: none"> Crumbs Complexe 				K22 XX
		Facies 3 <ul style="list-style-type: none"> Matrix Support <ul style="list-style-type: none"> Crumbs Complexe 		XIX,XX,XXI,XXIII, XXIV,XXVI,XXVII,XXVIII		K22 XX
		Variable Support <ul style="list-style-type: none"> Granular Crumbs Complexe 		xxxv		K22 XXXV

Figure 1: Synthetic trees of Microfacies Classification composing the columns N12, N16/N17 and K22 of Gran Dolina TD

AB gradation present inside TD- 10	Microfacies			B master horizon present inside TD-10	Microfacies			BC gradation present inside TD- 10	microfacies K22
	N12	N16/N17	K22		N12	N16/N17	K22		
AB-kk	XII to XVIII		III to IV	B-kk	XIX		I to II	BC-k	XXXII to XL
AB-kk-f	I to XI			B-kk-s-r	XXXVIII			BC-k-s	XLIV to XLV
AB-kk-f-s	XX to XXVII			B-kk-t-s			XII; XV to XVI; XX to XXIII	BC-k-s-t-f	LI to LII
AB-kk-f-t		I to IV		B-kk-f				BC-kk-t-s	XLII
AB-kk-t-s		XIII	XLVI to L	B-k-t-s			XXVI TO XXVIII		
AB-kk-t	XXIX	V to VI		B-k-t-r			XXIX		
AB-kk-s-e				B-k-t			XXXI		
AB-k	XL to XLI		XIII to XIV	B-k-f	VII to XII		V		
AB-k-t			XXX; XLI						
AB-k-t-e			XXIV to XXV						
AB-k-t-c		XIV to XX							
AB-k-s			XLIII						
AB-k-f-t			VI to XI						
AB-k-t-s-(f)			XVII to XIX						

Figure 2: List al all the types of Horizon find inside the TD-10-layer with the microfacies corresponding